

# **For Reference**

---

**NOT TO BE TAKEN FROM THIS ROOM**



Ex LIBRIS  
UNIVERSITATIS  
ALBERTAENSIS





Digitized by the Internet Archive  
in 2019 with funding from  
University of Alberta Libraries

<https://archive.org/details/Chaplin1981>





THE UNIVERSITY OF ALBERTA

RELEASE FORM

NAME OF AUTHOR                      CATHERINE E. CHAPLIN  
TITLE OF THESIS                      ISOTOPE GEOLOGY OF THE GLOSERHEIA  
   GRANITE PEGMATITE, SOUTH NORWAY  
DEGREE FOR WHICH THESIS WAS PRESENTED: MASTER OF SCIENCE  
YEAR THIS DEGREE GRANTED: 1981

Permission is hereby granted to the UNIVERSITY OF ALBERTA LIBRARY to reproduce single copies of this thesis and to lend or sell such copies for private, scholarly or scientific research purposes only.

The author reserves other publication rights, and neither the thesis nor extensive extracts from it may be printed or otherwise reproduced without the author's written permission.







THE UNIVERSITY OF ALBERTA

ISOTOPE GEOLOGY OF THE GLOSERHEIA  
GRANITE PEGMATITE, SOUTH NORWAY

by



CATHERINE E. CHAPLIN

A THESIS

SUBMITTED TO THE FACULTY OF GRADUATE STUDIES AND RESEARCH  
IN PARTIAL FULFILMENT OF THE REQUIREMENTS FOR THE DEGREE  
OF MASTER OF SCIENCE

DEPARTMENT OF GEOLOGY

EDMONTON, ALBERTA

SPRING, 1981







THE UNIVERSITY OF ALBERTA  
FACULTY OF GRADUATE STUDIES AND RESEARCH

The undersigned certify that they have read, and recommend to the Faculty of Graduate Studies and Research, for acceptance, a thesis entitled Isotope Geology of the Gloserheia Granite Pegmatite, South Norway, submitted by Catherine Chaplin, BSc., in partial fulfilment of the requirements for the degree of Master of Science.





## ABSTRACT

The mineral phases from a complex granitic pegmatite, the Gloserheia pegmatite of South Norway, were analysed for their U-Pb, Rb-Sr and oxygen isotopic composition. The pegmatite intrudes amphibolitic country rock of the Bamble sector of the Precambrian Baltic Shield within the time span of the Sveco-Norwegian orogeny (1100-1000 m.y.). The U-Pb concordia date of  $1055 \pm 30$  m.y. is taken to be the time of intrusion and crystallization of the pegmatite, while the later Rb-Sr mineral isochron date of  $1009 \pm 6$  m.y. is interpreted to be the time of the last major pulse of the Sveco-Norwegian event in that area of the Baltic Shield. The initial Sr isotope ratio and the  $^{18}\text{O}$ -enriched nature of the mineral phases suggests that the probable parent material for the pegmatite magma is the amphibolitic country rock that forms the predominant rock type in the area.

Considerable scatter of some of the Rb-Sr data and disequilibrium oxygen isotope fractionations of the silicate mineral phases can be correlated to alteration of (in particular) the feldspars, which suggests that an event subsequent to 1009 m.y. ago resulted in local open system isotopic redistribution. These effects have masked any isotopic distributions that might be expected to have developed during fractional crystallization from a silicate magma. On the whole, the data can be interpreted as supporting this model of pegmatite genesis.





## ACKNOWLEDGEMENTS

I wish to thank Dr. H. Baadsgaard for suggesting the project and for introducing me to the techniques of isotope dilution analysis and mass spectrometry. His advice and continual support throughout the study are greatly appreciated. The project originated from Dr. W. Griffin of the Mineralogisk-Geologisk Museum of Oslo, Norway. The samples were kindly provided by Dr. Griffin and his assistant J. Brommeland. Dr. R. St. J. Lambert's guidance during Dr. Baadsgaard's absence is gratefully remembered.

Thanks also go to Mrs. E. Toth, who prepared the samples for stable isotope analysis, and to Dr. K. Muehlenbachs, who performed the mass spectrometry. Dr. F. J. Longstaffe aided the interpretation of stable isotope results.

Mass spectrometry facilities in the Department of Physics of the University of Alberta were kindly provided by Dr. G. L. Cumming. D. Krstic will have ever a place in my heart for his ability to locate ion beams gone astray.

Dr. F. J. Longstaffe provided instruction for the operation of the X-ray fluorescence unit. Mr. A. Stelmach and Mr. L. W. Day provided assistance with the chemical preparations. Mr. D. McGrath prepared the thin sections.

Financial assistance was provided through University of Alberta bursaries and Graduate Teaching Assistantships.





# TABLE OF CONTENTS

	PAGE
ABSTRACT . . . . .	iv
ACKNOWLEDGEMENTS . . . . .	v
CHAPTER I. INTRODUCTION . . . . .	1
CHAPTER II PEGMATITES AND PEGMATITE FORMATION . . . . .	8
CHAPTER III. GEOLOGY . . . . .	17
Geology and geochronology of the Baltic Shield . . . . .	17
Geology and geochronology of the Bamble sector, South Norway. . . . .	19
Geology of the Gloserheia granite pegmatite . . . . .	23
CHAPTER IV. RUBIDIUM-STRONTIUM GEOCHRONOLOGY . . . . .	31
Introduction . . . . .	31
Rubidium-strontium isotope systematics . . . . .	31
Samples . . . . .	37
Analytical . . . . .	39
Results . . . . .	40
Discussion and conclusions . . . . .	46
CHAPTER V. URANIUM-LEAD GEOCHRONOLOGY . . . . .	53
Introduction . . . . .	53
Uranium-lead isotope systematics . . . . .	54
Samples . . . . .	56
Analytical . . . . .	58
Results . . . . .	60
Discussion and conclusions . . . . .	60
CHAPTER VI. OXYGEN ISOTOPE GEOCHEMISTRY . . . . .	66
Introduction . . . . .	66
Oxygen isotope systematics . . . . .	66





	PAGE
Samples . . . . .	73
Analytical . . . . .	74
Results . . . . .	74
Discussion and conclusions . . . . .	77
CHAPTER VII. SUMMARY AND CONCLUSIONS . . . . .	81
REFERENCES . . . . .	89
APPENDIX A. DESCRIPTION AND LOCATION OF SAMPLES . . . . .	96
APPENDIX B. MINERAL SEPARATION PROCEDURES . . . . .	108
APPENDIX C. ANALYTICAL TECHNIQUES . . . . .	109
i. Rubidium-strontium . . . . .	109
ii. Uranium-lead . . . . .	110





## LIST OF TABLES

	PAGE
TABLE 1. Mineral compositions of the different zones in the Gloserheia pegmatite.	26
TABLE 2. Rb/Sr analytical data for minerals from the Gloserheia pegmatite.	41
TABLE 3. U/Pb analytical data for minerals from the Gloserheia pegmatite.	61
TABLE 4. U/Pb apparent dates and analytical data for minerals from the Gloserheia pegmatite.	62
TABLE 5. $^{18}\text{O}/^{16}\text{O}$ ratios for minerals from the Gloserheia pegmatite.	75



## LIST OF FIGURES

	PAGE
FIGURE 1. Schematic geochronological map of the Baltic Shield.	18
FIGURE 2. Location of the Gloserheia pegmatite.	24
FIGURE 3. The shape of the Gloserheia pegmatite.	24
FIGURE 4. Plot of $^{87}\text{Sr}/^{86}\text{Sr}$ ratios versus $^{87}\text{Rb}/^{86}\text{Sr}$ ratios for feldspars from the Gloserheia pegmatite.	44
FIGURE 5. Plot of $^{87}\text{Sr}/^{86}\text{Sr}$ ratios versus $^{87}\text{Rb}/^{86}\text{Sr}$ ratios for biotites and muscovites from the Gloserheia pegmatite.	45
FIGURE 6. $^{206}\text{Pb}/^{238}\text{U}$ - $^{207}\text{Pb}/^{235}\text{U}$ Diagram for minerals from the Gloserheia pegmatite.	62
FIGURE 7. Oxygen isotope analyses of minerals in the Gloserheia pegmatite and surrounding amphibolite.	76
FIGURE 8. The Gloserheia pegmatite: map of quarry.	97





## CHAPTER I INTRODUCTION

The disintegration of naturally occurring radioactive nuclides results in isotopic variations that may be used to infer time relationships and processes affecting geological materials. Chronological methods developed prior to the advent of isotope geochronology are still useful, but have some limitations. Intrusive relationships and the law of superposition clarify relative sequences. Relative ages are obtained most often from fossils of the Phanerozoic, a comparatively short span of geologic time. Palaeontology and stratigraphy can be applied to correlation problems in the thin surface veneer of supracrustal sediments. None of these methods, however, allows a quantitative assessment of the time of formation or the subsequent metamorphic history of a body of rock.

The discovery of radioactivity by Bequerel opened the door to a quantitative assessment of geologic time. Because the rate of decay of a radioactive nuclide is fixed, the quantity and rate of decay of a radioactive 'parent' nuclide and the accumulated quantity of its radiogenic 'daughter' can be used to calculate the time elapsed since the mineral or rock became a chemically closed system.

A number of naturally-occurring radioactive nuclides exist. The suitability of a given parent-daughter pair for the determination of the age of a material depends on several important factors. A key consideration is the presence of a sufficient (ie. measurable) quantity of both the parent and the daughter nuclide. This in turn is in part governed by the time required for one half of a given number of radioactive parent nuclides to spontaneously disintegrate, termed the



'half-life'. For very old rocks, three 'nuclear clocks' are presently in common use: these are the parent-daughter pairs K-Ar and Rb-Sr, and the family U-Th-Pb.

A number of criteria, both analytical and geological, must be observed before significance can be attached to a mineral or rock date. Accurate determination of the rate of decay of the radioactive nuclide and of the abundance of the radioactive and radiogenic isotopes are essential. If an abundance ratio is used, the isotopic composition of the element must be known and constant in nature. These two requirements are essentially satisfied at the present time. It is more difficult to assess the degree of fulfillment of the next three criteria. The phase to be dated should be free of 'contaminant' daughter at the time of formation, or the amount of contaminant must be known and corrected for. The phase should act as a closed system after the event of interest; specifically, no gain or loss of parent or daughter nuclide should occur. Lastly, the geological field relationships of the sample must be well known so that the phase chosen for dating is representative of the event of interest.

If all of these criteria are satisfied, the date becomes an age for a given mineral or rock. However, no parent-daughter combination typifies ideal behavior, and natural systems may be affected by a complex array of variables. The nuclides of interest are generally not major constituents of mineral lattices, and they may be selectively gained or lost without causing reconstitution or even disruption of the lattice (Giletti, 1974). Violation of any one of these criteria may not be apparent without an independent check. The best single check is the application of another decay scheme to a coexisting mineral. Discordant





ages indicate that at least one of the criteria has not been satisfied.

The most basic difficulty is undoubtedly the assessment of the degree of closed system behavior of a rock or mineral between the time of formation and the present. Yet it is the very failure to behave ideally that can contribute a wealth of information to the understanding of geological processes that may affect a mineral phase during its residence in the Earth's crust. This is a two-fold problem. To unravel the history of a given mineral the geochronologist must not only be familiar with the type of events that result in open system behavior, but also with the different mechanisms on the molecular level that allow for loss, gain, or exchange of a particular nuclide in response to a particular event. The geological events that result in open system behavior are well known, and may be loosely grouped as 'metamorphic' or 'weathering' processes. In response, chemical reaction, recrystallization and diffusion all result in at least transient open system behavior, allowing loss or gain of nuclides. The behavior of the different elements that comprise the various parent-daughter pairs are governed by two factors: the inherent geochemical characteristics of an element, and the differential responses of the environment -the mineral lattice- in which the nuclide resides, to changes in physical and chemical conditions that affect equilibrium relationships. The remaining challenge involves reliably linking the 'cause' and 'effect' relationships.

Significant differences in age are often shown by cogenetic minerals. From studies of systems showing such relationships, schemes were devised to interpret discordant ages, most importantly, Nicolaysen's (1961) rubidium-strontium isochron plot, and the uranium-lead concordia



plot originated by Wetherill (1956) and refined by Tilton (1960). These graphical representations are essentially independent of the mechanism of loss: they only indicate the age of a rock or mineral system, and the time of an episode of open system behavior for a mineral. Attention has been subsequently directed to the cause of this open system behavior. One example is a classic study by Hart (1964) of the effect of the intrusion of the Eldora stock into the Precambrian of the Colorado Rockies. This study is a detailed account of the isotopic response of several common silicate minerals to temperature in an essentially single-variable natural experiment. Numerous other studies of this type have been published since. At the same time, growing attention has been directed towards mechanisms on an atomic level, such as those described in a recently published volume entitled "Geochemical Transport and Kinetics" (Hofmann et al, 1974).

As the awareness of the importance of these processes grows, increasing attention is being given by geochronologists to the behavior of other nuclides, or specifically, stable isotopes. Oxygen isotopes have received the greatest attention, for oxygen is abundant in common rock forming minerals, and the factors that govern the distribution and fractionation of its isotopes in natural systems are well understood.

The comparative study of strontium and oxygen isotopes is of particular importance. A considerable quantity of literature exists that concerns the use of contaminant radiogenic strontium in a mineral phase as a petrogenetic indicator. At the same time, an equal volume of literature has established oxygen isotopic composition as a petrogenetic indicator in its own right. The factors that control the enrichment of  $^{87}\text{Sr}$  and  $^{18}\text{O}$  in the crust are the result of two completely





different mechanisms. Combination of the two together can remove much of the usual ambiguity in an interpretation based on one system alone, and it can become possible to determine the origin of a magma and its degree of interaction with pre-existing crustal material.

Of all of the methods presently available, oxygen isotopes are probably the most powerful tool that can be used to consider the processes that affect a mineral phase subsequent to its crystallization. Fractionation effects, because they depend mostly on differences in isotopic weight, are much more pronounced for isotopes of oxygen than strontium (or most other common mineral forming nuclides). Conveniently, oxygen isotope fractionation is greatest at low temperatures, so that many of the geological events that result in isotopic exchange and redistribution can be simulated and studied with ease in the laboratory. As a result, these processes are relatively well understood. In comparison, the behavior of strontium isotopes can only be studied in the context of their environment, and these responses, dictated by mineral lattice stability, most commonly occur at high temperature and pressure conditions that are difficult to reproduce in the laboratory. Many laboratory results have not been perfectly satisfactory, so in order to study such processes, another approach is often chosen. This involves study in a 'natural' laboratory, similar to Hart's (1964) investigation. Rocks are complex systems, and in order to comprehend the response of a system to a geologic event, the response of each separate component of the system (ie. each mineral phase) must be known. At the present time, enough uncertainty still exists that for an experiment to be suitable, most of the variables must be accurately known and controlled.

With due consideration given to all of these principles and



parameters, a project was selected to assess the application of the basic principles of geochronology to a natural system, and at the same time contribute useful geological information. The Gloserheia complex pegmatite, from South Norway, was selected on the basis of several considerations. Complex pegmatite genesis is a problem of basic significance to igneous petrology, because it is believed to be related to the end stage of magmatic crystallization; and because it is believed to form a telescoped representation of fractional crystallization. It is also of importance to economic geology, because pegmatites are the sole economic source of many unusual elements and minerals. Yet pegmatites have received relatively little attention in the post war years, and references to the isotopic composition may be tallied on one hand. Pegmatites are well-suited to isotopic study. They commonly contain minerals with relatively high concentrations of the radioactive parent nuclides Rb, U, Th, and K, and at the same time have abundant, well distributed oxygen-bearing silicate phases. Pegmatite bodies are small enough to study with ease, but afford sufficient internal compositional variation to be interesting. If the pegmatite has been quarried, relatively unweathered samples for analysis may be obtained. There is some contention regarding both the genesis of pegmatites and the source of their mineralization, with some models requiring open system addition of mineral components, while other models require single stage emplacement. They are thus ideal candidates for the study of isotopic response to open system behavior. The Gloserheia pegmatite was studied for variation in Rb-Sr, U-Pb and  $^{18}\text{O}/^{16}\text{O}$  composition related to the pronounced structural zoning exhibited by this and most other complex pegmatites. The experimental results were considered in terms





of assigning a time of formation to the pegmatite, a source for the magma from which it crystallized, and the cause and effect relationships of the open system behavior which contributed to the final product that now exists.



## CHAPTER II PEGMATITES AND PEGMATITE FORMATION

Pegmatites are small, intrusive, usually coarse-grained holocrystalline bodies. They are dominantly composed of quartz and feldspar, and often contain highly variable and exotic accessory minerals. Pegmatites have been divided into two broad classes on the basis of proposed origin. The most common class, simple or 'sweat' pegmatites, are believed to be metamorphic in origin. They are characterized by small size (up to several meters across), relatively fine grain size, and simple mineral assemblages. Pegmatites believed to be of igneous origin may be simple or complex. Complex pegmatites, a group to which the Glosseheia pegmatite belongs, are relatively uncommon. Complex pegmatites are large in size in comparison to simple pegmatites (ie. up to tens of meters across), are quite coarse grained, and often have widely varied and unusual mineral assemblages. Comprehensive descriptions of the variations in geometry and mineral assemblages observed in complex pegmatites have been published by Cameron et al (1949), Jahns (1953, 1955) and Brøtzen (1959).

Complex pegmatites are characteristically zoned. The zones are systematically arranged and are lithologically distinct units. They are expressed by variations in mineral distribution and in grain size. Within a single pegmatite, grain size may range from millimeters to tens of meters, increasing towards the center. There is a corresponding increase in the complexity of the mineral assemblages, with the more exotic minerals concentrated in the inner regions. The zones are concentrically disposed and to variable degrees reflect the size, shape and structure of the body. They grade from uniform, continuous units to



discontinuous pods or lenses. The number of zones in any given pegmatite is highly variable, ranging from one to over eleven.

Cameron et al (1949) proposed a structural division of complex pegmatites into border, wall, intermediate and core zones. The border zone is the narrow, fine-grained aplitic selvage. Contacts with the enclosing country rock are commonly sharp. The wall zone, next adjacent, is characteristically thicker and coarser-grained. The core is an elongate lens or series of pods centered within the body. Zones between the core and the wall zone are designated as intermediate zones and are signified by a letter or number increasing away from the core.

The border and wall zones are mineralogically similar. They are composed of fine-grained aplitic or graphic intergrowths of quartz and feldspar. These two zones are generally completely and continuously developed.

Intermediate zones are often incompletely and asymmetrically developed. Inter-zone contacts range from gradational to sharp, and 'telescoping' of units is common. One or all of the zones may be entirely absent, with zones ranging in number from zero to greater than five. Usually five intermediate zones are present. The mineralogy is more variable than the wall zone, for the widely variable suites of accessory minerals are concentrated here. The major constituents are oligoclase, microcline, quartz and biotite. Early-forming rare-earth minerals are characteristically found attached to or enclosed by plates of biotite. Textures range from subhedral to euhedral, and the already coarse grain size commonly increases towards the core.

The core is generally symmetrically located with respect to the sides of the pegmatite, and frequently closely reflects the external





shape. The core may be composed entirely of quartz or contain subordinate amounts of feldspar (usually microcline) and mica. Crystals may be extremely large and may range in texture from anhedral to euhedral. 'Giant' pegmatitic textures, when present, are found in the core and the innermost intermediate zones.

'Magmatic' pegmatites have been subdivided into four groups on the basis of accessory mineral assemblages (Brotzen, 1959), ie. pegmatites bearing:

- (1) oxides; eg. columbite, samarskite, cassiterite, euxenite.
- (2) phosphates and fluorides; eg. monazite, fluorite, apatite, Li-Na-Mn-Fe phosphates.
- (3) aluminosilicates, with small highly charged cations; eg. beryl, tourmaline.
- (4) aluminosilicates, with small cations of unit charge; eg. albite, spodumene.

Pegmatites emplaced in the same region often have the same suite of accessory minerals.

Basic features of granitic pegmatites are often found to have superimposed complicating features. These features appear to be functions of the degree of alteration and replacement. Brotzen (1959) has qualitatively classified these according to the stage in development. The most common feature is the addition of muscovite, which may be abundant and can occur independently of other late mineralization. The appearance of muscovite signifies the increased activity of water. It may crystallize directly or form through the partial hydrolysis of microcline. In the second stage, muscovite is frequently associated with sugary albite in fracture fillings and forms a replacement for microcline.



This albite replacement tends to obliterate the original zoning. Mineralization is characteristically associated with these veins and patches. Late lithium (and/or subordinate phosphate, cesium and sodium) mineralization represents the most advanced stage of replacement, and is represented by the presence of lepidolite, amblygonite, and spodumene in addition to muscovite and albite. These late mineralizations, with the exception of muscovite, are localized between the quartz core and the microcline-bearing intermediate zone.

Controversy regarding the mechanism of formation of pegmatites is long standing. The mode of emplacement, the source of material, and the physical and chemical conditions of crystallization have all been the subject of speculation. Early scientists suggested that pegmatites crystallized from the walls inwards in an open channelway. Successive fluids of different chemical composition precipitated the various layers or zones of a pegmatite, similar to the behavior of ore-bearing hydrothermal fluids in a major shear zone. Textural relationships coupled with an improved understanding of magmatic and metasomatic processes have caused this early hypothesis to be essentially abandoned.

The common alteration and replacement of minerals has led many geologists to propose a replacement origin for pegmatites. Commonly cited evidence for metasomatic or replacement origin includes:

- (1) clear evidence of post-consolidation replacement; with pseudomorphism, transection and corrosion of early minerals. Channels lined with subhedral crystals are commonly observed to crosscut earlier minerals or rocks.
- (2) the presence of giant crystals poses serious problems of support during growth from a magma or fluid, as does the presence of





stellate, three-dimensional aggregates of prismatic minerals.

- (3) discrepancies between the composition of zones and the composition expected to have formed from a magma crystallizing in an essentially closed system whose liquid phase was yielding only crystalline material.
- (4) simple fractional crystallization cannot satisfactorily account for a quartz core or for the essentially monomineralic microcline zone usually found adjacent to it. In the final stages of (simple) fractional crystallization, plagioclase and microcline should consolidate at a partial eutectic.
- (5) in many cases, there is insufficient muscovite to act as a repository for potassium liberated during late albite replacement of microcline. A potassium imbalance results.

Certain authors (dominantly proponents of metasomatism) prefer a single genesis for all pegmatites and regard the textures and degree of internal (zonal) segregation as a function of the size of the body. For example, Gresens (1967) has proposed interaction of an alkali chloride fluid phase with pre-existing quartz-muscovite schist in a tectonically induced low pressure zone. The quartz core is the first part of the pegmatite to form as a result of recrystallization of migrating silica. This is succeeded by feldspar recrystallization. Late replacement muscovite forms when lithostatic pressure is re-established, making the feldspar unstable. Rare or trace elements concentrate to form exotic minerals during expulsion from mineral lattices during re-ordering and recrystallization, or they may be hydrothermally introduced. Reitan (1965) suggested secondary recrystallization of a relatively few grains of aplite to consume surrounding grains. This



reaction is driven by the reduction of total grain boundary free energy, in a process similar to metallurgical annealing.

Although these and other similar models suffice for some pegmatite occurrences, they fail to account adequately for the features observed in many others. The most recent model of pegmatite genesis is magmatic, and concerns itself only with complex pegmatites. There is a growing body of isotopic and geothermometric evidence to support this now widely accepted model. Jahns and Burham (1969) proposed that pegmatites develop in situ in an essentially closed chamber, under 'restricted system' conditions; that is, there is no new addition of magma, but the existing magma may freely exchange with the surrounding country rock. Internal zoning develops from the walls inwards in response to fractional crystallization of the magma, with incomplete reaction between the crystals and the rest liquid.

The magma may be either primary igneous or the result of local anatexis of crustal material. The only requirement is that the starting material be rich in dissolved volatiles, especially water. Exchange between the magma and the wall rock is to be expected, but for the sake of simplicity the system is otherwise regarded as closed.

Crystallization of the magma could commence anywhere in the range 1300-650°C. In natural systems, considerable ranges in the liquidus temperature result from variations in the confining pressure, the anhydrous composition, and the quantity and composition of the volatiles present. Crystallization, with or without reaction between the crystals and the silicate melt, would gradually lead to saturation of the melt with volatiles, and hence to the phenomenon known as resurgent or retrograde boiling. The appearance of a second fluid phase is regarded



as a key condition. It can be correlated to the development of intermediate zones and the core, and typical pegmatite textures, such as giant crystals, large scale mineral replacement and pseudomorphism. The inward increase in grain size in pegmatites is usually not observed to be gradual. Rather, there is an abrupt increase in one of the outer intermediate zones, and Jahns and Burnham attribute this to the appearance of the second fluid phase.

The fluid would initially separate on a submicroscopic scale. The "bubbles" of this immiscible liquid would coalesce and assume the role of an interstitial fluid. Most likely it would be in a supercritical state with respect to both pressure and temperature. The two phases would differ in composition and in physical properties. Diffusion of material in the much less viscous aqueous phase could be expected to occur as much as eight to ten orders more rapidly, facilitating the formation of large crystals and the reaction and corrosion of early-formed crystals no longer in equilibrium.

Both the textural and mineralogical variations that represent zones have been attributed to the presence of a second fluid phase. Quantities of dilute fluid would enhance transfer of relatively non-volatile material, either through fluid movement, or more likely, through diffusion in the fluid in response to a compositional gradient. Thermal gradients are to be expected in cooling igneous bodies. They have been demonstrated to induce compositional gradients for various constituents with differing temperature-dependent solubilities and/or rates of diffusion. In other words, the partitioning of materials between the silicate magma and the aqueous phase and the rate of movement of this material through the aqueous phase can differ considerably for different





constituents. Partitioning of material between the two fluids is of course never perfect. Nonetheless, the aqueous fluid exhibits a marked preference for potassium and lithium, while the magma tends to concentrate soda-bearing phases. The compositional sum of both components is roughly equivalent to crystallization from a silicate melt in the absence of a free aqueous phase.

The degree of segregation of minerals becomes more marked as the volume and degree of interconnection of the aqueous fluid increases. The aqueous fluid produces either segregated masses or pockets of potassium feldspar and muscovite. The pockets, interstitial to or within aggregates of large crystals, form in response to limited coalescence of the fluid bubbles. Gross segregation of potassic minerals from sodic plagioclase (ie., in the inner intermediate zones) is related to the preferential transfer of potassium relative to sodium in the aqueous fluid. Silica that is not being fixed in the aluminosilicates is segregated to varying degrees by transfer through the aqueous phase and crystallizes as coarse-grained quartz in the final stages.

The problem of support during crystallization from a liquid for very large crystals and radial, three dimensional aggregates has often been raised as an objection to magmatic origin. These crystals could not have grown in a liquid without some means of support. In response to this Jahns (1953) suggested that two or more minerals may crystallize penecontemporaneously to form a loose mesh providing a delicate support. Quartz appears to have developed with or slightly after the other minerals, filling the interstices and healing basal fractures (which are simple tensional breaks, rather than a phenomenon caused by replacement) in elongate prismatic minerals.



As crystallization continues, the silicate liquid would most likely be used up before the coexisting aqueous phase. At this point the aqueous phase would no longer be supercritical, at least with respect to temperature, and condense to a liquid and a vapor. Theoretically the three phases could coexist, but only under very unusual geological conditions. The amount of the liquid and vapor would be small, but could well be highly corrosive with respect to the early formed crystalline phases, resulting in widespread reaction and replacement. These reactions would be responsible for features such as partial or complete crystal pseudomorphs, aggregates of coarse-grained sodic albite, and the crystallization of typical 'pocket' minerals such as carbonate, members of the epidote group, and sheet structure minerals. Reaction and recrystallization would continue until all of the fluids are used up, and the final temperature of crystallization could well extend down to the hydrothermal or hypogene (100°C) range.

Reduction in the total confining pressure could happen at any stage during crystallization. This might occur through fracturing of the country rock with attendant rapid loss of volatiles. This loss is selective, favouring potash over soda and alkalies over silica and alumina, and produces metasomatic alteration of the host rocks. This would also rapidly move the system into the subsolidus region and cause quenching of the crystallizing silicate liquid. Typical development of aplite in small to large veins or fracture fillings is accounted for in this manner.





### CHAPTER III GEOLOGY

The material for this study comes from a single pegmatite body located at Gloserheia, South Norway. The pegmatite is located in the Bamble sector of the Precambrian Baltic Shield. It is apparently either the product of anatexis of the amphibolitic country rock, or a direct mantle derivative. The age of the pegmatite is unknown. An isotopic study is perhaps the best approach to obtain direct solutions to the questions of origin and age. If this information may be obtained, the pegmatite and the events leading to its formation can be related to the geological history of this sector of the Baltic Shield.

#### GEOLOGY AND GEOCHRONOLOGY OF THE BALTIC SHIELD

The Baltic Shield's main structural features are believed to have evolved continuously in an asymmetric pattern through the Archean and Early Proterozoic. The Early to Middle Proterozoic, marked by a period of consolidation and deposition of continental sediments, was followed by late Middle Proterozoic orogenesis discordant to earlier structural patterns. Post-Precambrian sediments, intrusives, and deep crustal faulting have resulted in only minor modification of pre-existing structures.

A great many Baltic Shield age determinations have been published, most notably by Neumann (1960), Polkanov and Gerling (1961) and Broch (1964). In a cumulative survey, Kratz et al (1968) outlined a now widely accepted isotopic division of the Shield into three major zones (see Figure 1). These subdivisions are in good agreement with present understanding of the structural and geophysical trends.

The eastern area of the Shield, known as the Karelides, or the



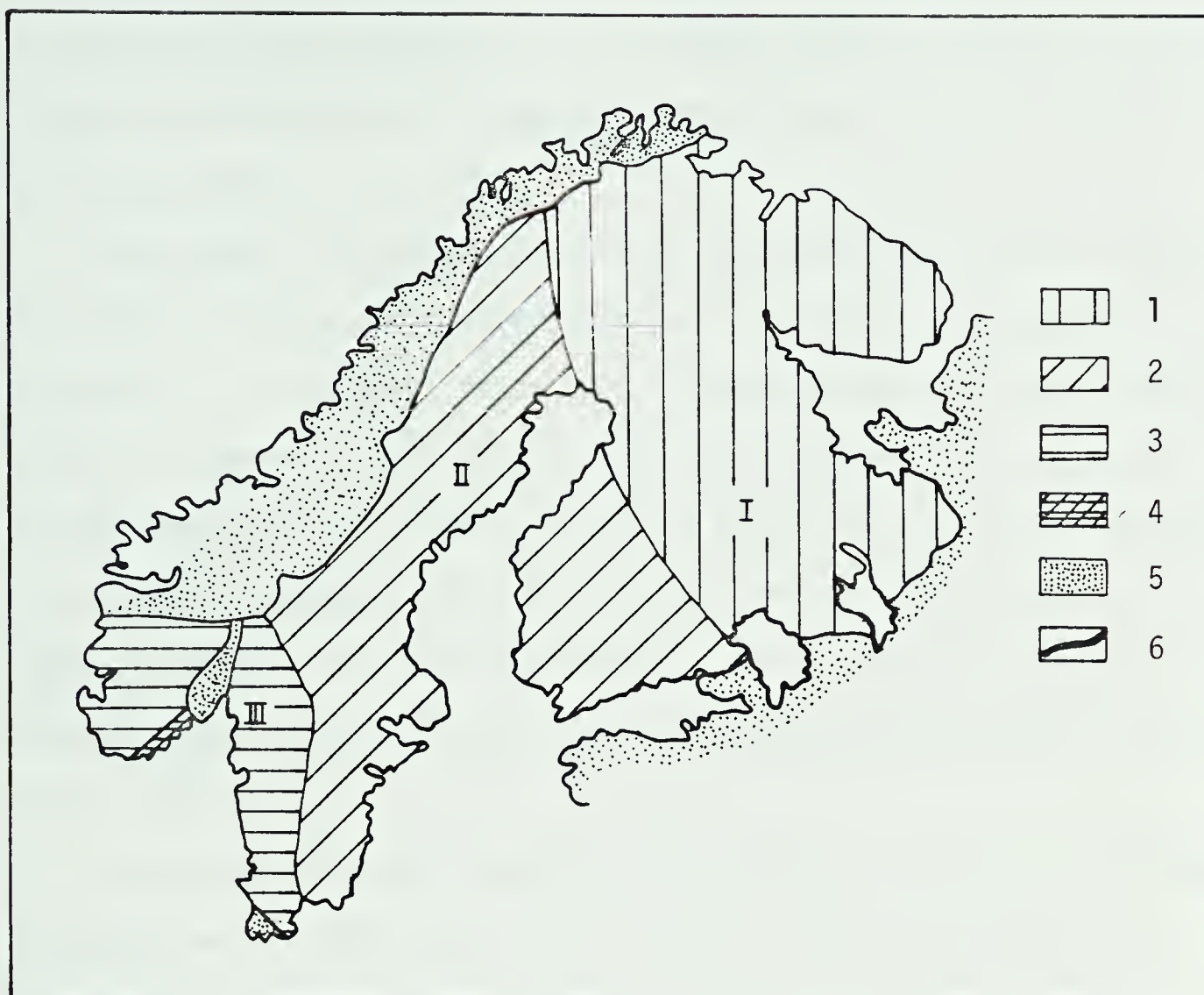


Figure 1. Schematic geochronological map of the Baltic Shield. Geochronological zones: I=Sammo-Karelian; II=Sveco-Fennian; and III=Sveco-Norwegian. Orogenic formations with age: 1=3600-1900 m.y.; 2=2300-1650 m.y.; 3=1200-900 m.y. 4=Bamble sector; 5=Eocambrian and Paleozoic; 6=boundaries of zones. After Kratz et al, 1968.



Saamo-Karelian Zone, is the most ancient, with ages ranging from 3600 to 1900 m.y. Main structural features evolved in the Archean and Early Proterozoic with the formation of granulite terrains. The Middle Proterozoic (1900 to 1650 m.y.) of the Saamo-Karelian Zone was characterized by an epigeosynclinal subplatform environment. Crustal thicknesses are approximately 34 to 38 km.

The central and western Shield, or the Sveco-Fennian Zone, consists dominantly of Early and Middle Proterozoic supracrustal and plutonic formations. The basement is unknown. Intense orogeny between 1950 and 1700 m.y. appears to have obliterated much of the earlier structure. Crustal thicknesses are approximately 39 to 42 km. The isotopic boundary to the north coincides with a deep-seated vertical crustal zone. The western boundary (with the Sveco-Fennian Zone) is marked geologically by a major fault with associated hyperite (olivine-bearing norite) intrusives dating 1000 m.y.

The extreme southwest portion of the Shield, or the Sveco-Norwegian Zone, has relic older ages of 1550-1700 m.y., with superimposed structurally discordant ages of mainly 1000 m.y. or less. Crustal thicknesses are approximately 36 to 38 km.

#### GEOLOGY AND GEOCHRONOLOGY OF THE BAMBLE SECTOR, SOUTH NORWAY

The Sveco-Norwegian Zone has been subdivided into a number of sectors. The area of principal concern is the Bamble sector, which lies between Langesund and Kristiansand in the Skagerrak coastal region of South Norway.

Regional geological descriptions of this area have been published by Bugge (1943), O'Nions et al (1969), O'Nions and Baadsgaard (1971), and Field and Råheim (1979). Geological boundaries of the Bamble





sector are, to the east, Cambro-Silurian sediments, and a proposed fault offshore of the Skaergård islands (O'Nions, 1969); and to the west, the Porsgrunn-Kristiansand fault. This major NE-SW shear zone, extending from Porsgrunn south to the coastal town of Kristiansand, is marked by an approximately 4 km. wide band of cataclastics. O'Nions (1969) postulates that this down-faulted block, known as the Bamble-Kristiansand sector, represents a southwestern extension of the Oslo graben.

The geological assemblage is of essentially sedimentary and volcanic origin metamorphosed to dominantly upper amphibolite facies assemblages. Major rock types are interbedded quartzites, biotite-hornblende schists, amphibolites, granites, granodiorites, and quartz-diorite gneisses. Less dominant are marbles, calcsilicate rocks, and anthophyllite cordierite rocks.

The bulk of the terrain is composed of relatively old (approximately 1700 m.y.) volcanics and sediments metamorphosed to the sillimanite-almandine-orthoclase subfacies of the almandine-amphibolite facies. The metamorphic grade increases to the southwest towards the Arendal district, where hornblende and orthopyroxene granulites are found.

Conformable bands and boudins of amphibolites have textures and bulk chemistry consistent with igneous origin. Granitic gneisses occur as roughly lenticular bodies with igneous textures and poorly developed foliation. Compositional variations grading to granodiorite are found adjacent to amphibolites and biotite schists. The amphibolite facies gneisses have generally not been subdivided for mapping purposes. An exception is the synkinematic Levang granite gneiss, a NE-SW elongate medium-grained biotite granite with a broad domal structure. Field relations suggest a high grade in situ origin as the result of partial



anatexis.

Late and post-kinematic granites and hyperites intrude the gneisses. Field studies (O'Nions, 1969) and K-Ar and Rb-Sr geochronology (O'Nions et al, 1969; Field and Råheim, 1979) relate these to several pulses of activity between 1100 and 1000 m.y. This event has frequently been correlated with the Grenville of N. A. Reactivation of the Levang granite gneiss and emplacement of concordant plagioclase pegmatites was followed by the emplacement of hyperite, discordant granite sheets, and potassium feldspar pegmatites. The Grimstad and Herefoss granites, in the southern part of the sector, have been variously classified as synkinematic, based on one K-Ar age (reported by Neumann, 1960), and more recently post-kinematic, by field relationships (Bugge, 1943) and K-Ar geochronology (O'Nions, 1969), indicating an age of 860 m.y. for the Grimstad granite.

O'Nions (1969) describes two types of pegmatites, small in size ( $\leq 2$  m.) but ubiquitous throughout the Bamble sector. The plagioclase pegmatites are mineralogically simple, composed of quartz, plagioclase ( $An_{20}-An_{30}$ ), and biotite, with occasional sphene, rutile, diopside, and allanite. They are concordant with country rock foliation and are synkinematic, postulated to be the result of local partial anatexis related to the reactivation of the Levang granite gneiss. Discordant potassium feldspar pegmatites, composed of microcline, quartz, biotite, and muscovite are post-kinematic (approximately 1040 m.y.) and associated with the emplacement of small ( $\leq 30$  m.) granite sheets. These pegmatites frequently show enrichment in U, Th, Zr, Nb, Ta, and Ce, manifested in the appearance of allanite, zircon, sphene, and euxenite. These are interpreted to represent mobilized partial anatectic material.





Oftedal (1954) and Heier and Taylor (1959) have described a third group of pegmatites, larger in size and with anomalously low lead content. Two examples cited were the pegmatites at Arendal and Kragerø.

Later tectonic activity has been suggested by Neumann (1960), who reported a K-Ar age of 874 m.y. from a pegmatite at Vik, near Grimstad. Limited Permian (Caledonian) activity is manifested in iron-nickel-copper mineralization, dated by the common lead method, and in numerous NNW-SSE trending syenite and dolerite dikes. These are undated but inferred to be Permian in age (O'Nions, 1969).

A recent detailed Rb-Sr study of the Arendal region, published by Field and Råheim (1979) has resulted in re-evaluation of the significance of the 1600 and 1060 m.y. events, and additionally cast light on the nature of the quartzofeldspathic gneisses. These high iron, acid-intermediate orthogneisses can be chemically subdivided into two zones; one highly deficient in K and Rb ( $K_2O \sim 0.5\%$ ,  $Rb \sim 8$  ppm,  $Rb/Sr \sim 0.05$ ,  $K/Rb \sim 1300$ ) in contrast to a 'normal' upper crustal type ( $K_2O \sim 4\%$ ,  $Rb \sim 150$  ppm,  $Rb/Sr \sim 1.2$ ,  $K/Rb \sim 290$ ). An interpretation consistent with trace element modeling involves the separation of a potassium-poor cumulate phase from a magma directly emplaced under high grade conditions. The residual liquids crystallized as normal potassium charnockites. The metamorphic grade and the corresponding degree of dehydration related to this event are observed to increase from the NW towards the SE, climaxing in the environs of Arendal.

The sole identifiable secondary effect is trace hydration along minor irregularly spaced fractures related to a later series of undeformed subvertical intrusive granite sheets and pegmatite dikes. In the charnockites this event is manifested by the local replacement of



orthopyroxene by serpentine, chlorite and actinolite, secondary biotite growth and incipient turbidity in plagioclase.

Total rock Rb-Sr geochronology based on collection of a number of closely spaced samples in twelve localities yielded two distinct age groups at 1450-1550 m.y. and 1000-1100 m.y. Mineral isochrons for the same samples of both these groups give ages of 1040 m.y. The younger whole rock age of 1060 m.y. is associated with those localities showing relatively intense secondary alteration. The older whole rock age is obtained from localities completely lacking evidence of secondary effects. Ages intermediate to the two events are suggested to result from local open system behavior with partial isotope rehomogenization. No relationship to the alkali element chemistry was observed. Field and R  heim conclude that indiscriminate sampling of widely spaced (reset) localities have created an illusion of major regional isotope rehomogenization, when in fact quite different results are observed in closely spaced, carefully chosen localities. Thus in contradiction to the conclusions of O'Nions (1969) the 1060 m.y. event was minor in scale and as such should not be correlated with the Grenville event in the Canadian Shield.

#### GEOLOGY OF THE GLOSERHEIA GRANITE PEGMATITE

The Gloserheia pegmatite is located 9 km. north of Arendal, Norway ( $8^{\circ}43'36''\text{E}$ ,  $58^{\circ}32'20''\text{N}$ ) in the Bamble sector of the Precambrian Baltic Shield (see Figure 2). It has been intruded into upper amphibolite and granulite facies metasediments. The pegmatite has been previously briefly mentioned in geological reports by Anderson (1926, 1931) and Oftedal (1954). Heier and Taylor (1959), in a regional study of alkali trace element geochemistry, briefly compared the Gloserheia pegmatite



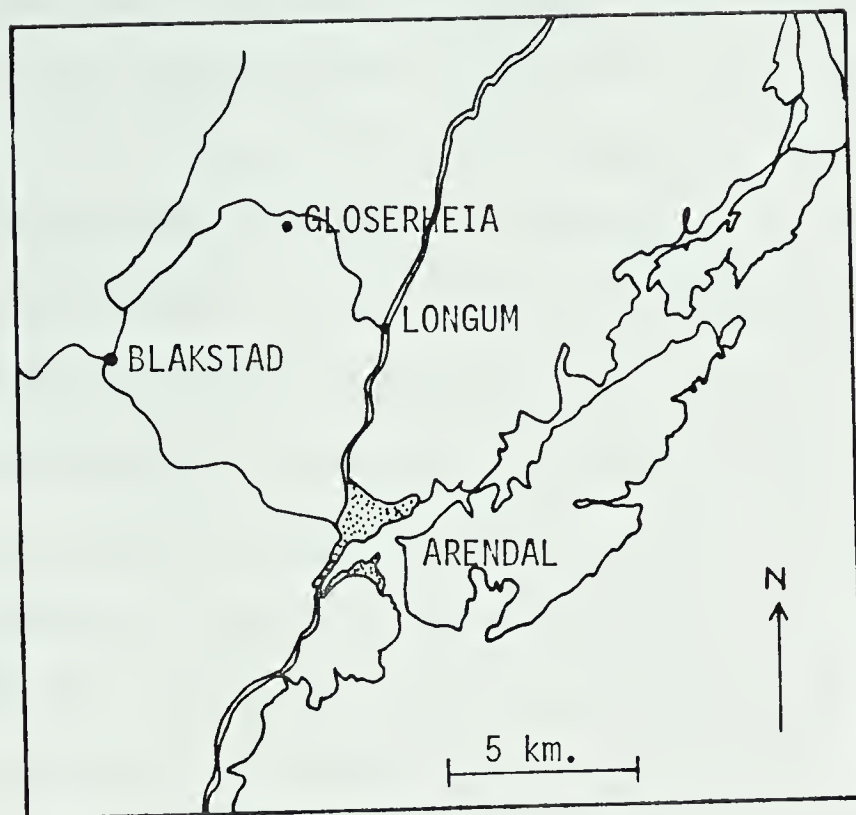


Figure 2. Location of the Gloserheia pegmatite.  
(after Åmli, 1977).

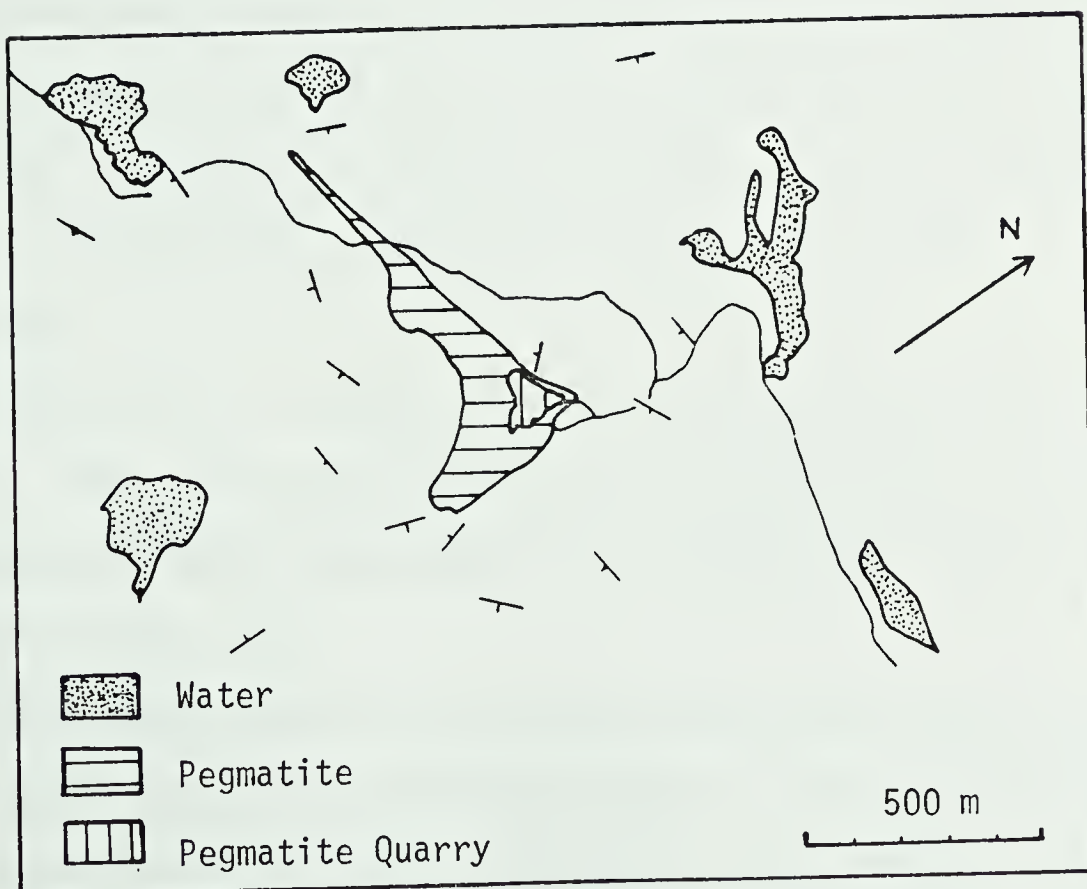


Figure 3. The shape of the Gloserheia pegmatite.  
(after Åmli, 1977).





to another found near Kragerø and commented on the anomalously low lead content of both. More recently, Åmli (1975, 1977) has published studies of the mineralogy and rare earth geochemistry of apatite and xenotime and of the internal structure and mineralogy of the pegmatite.

Åmli (1977) describes the pegmatite as a V-shaped body cross-cutting the country rock with generally smooth, sharp contacts (see Figure 3). Unfortunately the exposure in the area is poor and heavy overburden obscures most of the field relationships. The west arm of the body is observed to thin out and disappear under the overburden. The south arm terminates irregularly with interfingering gneisses. Evidence of stress includes bent twin lamellae in plagioclase, curved cleavage planes in muscovite, the development of a second fair cleavage in biotite, variable degrees of undulatory extinction in the major minerals and scattered microfracturing. The source of this strain may be related either to competing crystallization or to small-scale country rock deformation. Accordingly the pegmatite may be either syn- or post-tectonic. The pegmatite is described as unique in the area.

## 1. Structure

The quartz core is located in the northwest portion of the pegmatite. This is the only portion of the pegmatite that is relatively well exposed and Åmli's observations and interpretations of the zonal sequences are based here.

The Gloserheia pegmatite exhibits well developed, regular zoning. It has a quartz core, five intermediate zones, a wall zone and a border zone. Table 1 shows the mineral composition of the different zones.

The core in places is as much as 80 m. in width. It is almost entirely composed of dense masses of coarse-grained quartz. Occasional



TABLE 1. Mineral Composition of the Different Zones in the Gloserheia Pegmatite (after Åmli, 1977).

Mineral	Core zone	Int. zone I	Int. zone II	Int. zone III	Int. zone IV	Int. zone V	Wall Zone	Border zone
Quartz	M	A	T	A	M	M	M	M
Microcline	T	M		A	A	M	A	
Plagioclase			M	M	M	A	M	M
Biotite		A	T	A	A	A	A	A
Muscovite		A	A/T	A/T	T	T	T	T
Tourmaline	T	T		T				
Allanite		T		T				T
Apatite	T	T		T				
Euxenite		T		T			T	
Calcite		T	T	T				
Pyrite	T	T		T				
Magnetite		T					T	T
Rutile	T	T		T				
Xenotime	T	T		T				
Zircon				T				
Yttrotitanite				T				
Goethite	T	T		T				
Chlorite				T				
β-uranophane				T				
Uranophane				T				
Kasolite				T				
Uraninite				T				
Thorite		T		T				
Monazite	T	T						
Hematite		T						
Beryl			T	T				
Fourmarierite				T				

M: Main mineral. A: Accessory mineral. T: Trace mineral.





miarolitic druses are found, and there is a minor quantity of microcline. The contact with intermediate zone I is irregular because of the large size of the crystals.

The first intermediate zone varies in thickness from 0.5 to 3 m. Biotite and quartz are intersititial to blocky microcline. Biotite forms a narrow seam along the contact with the core zone.

Intermediate zone II is an essentially monomineralic zone of medium to coarse-grained anhedral plagioclase. The thickness of this zone varies from several dm. to about 1 m.

Intermediate zone III is characterized by the abundance of trace minerals. These include euxenite, allanite, biotite, apatite, zircon, uranophane, etc. Quartz, microcline, biotite, and euxenite occur throughout the zone. The other accessory minerals are localized in the areas of pronounced muscovitization. Thickness of the zone is about 1 dm.

Intermediate zone IV is composed of graphically intergrown plagioclase and quartz. At the contact with intermediate zone III the plagioclase is graphically intergrown in a similar texture with microcline. Thickness of the zone is about 1 dm.

Intermediate zone V is composed of graphically intergrown quartz and microcline. In places it is in contact with intermediate zone III, and in these locations a cm. size rim of microcline is present. The border with intermediate zone IV is locally myrmekitic. Patches of graphic-textured plagioclase and quartz and meter-sized areas of concentrically zoned quartz, microcline and plagioclase (from the center to the edge) are found sporadically. Zone V varies in thickness from 5 to 8 m.

The wall zone varies in thickness from 1 dm. to 1.5 m. The grain



size varies from 1 to 10 cm., and the texture is hypidiomorphic granular or locally aplitic. Mineralogy consists of graphically intergrown microcline or (dominantly) oligoclase and quartz, along with minor biotite, euxenite, and uranium secondary minerals.

The border zone is similar to the wall zone, but it is slightly enriched in magnetite and biotite.

## 2. Mineralogy

Quartz is the dominant mineral phase in the pegmatite. It is found in every zone, but is concentrated in the core zone. In the core, the quartz forms dense subhedral to anhedral masses. Usually it is translucent or milky in colour, but rose and smoky varieties are present in small quantities. In thin section, the quartz shows undulatory extinction, suggesting that it has been strained during or after crystallization. Small to medium-grained crystals of quartz are found elsewhere in the pegmatite in druses in altered parts of microcline crystals and as anhedral grains of variable size.

Microcline is the second most common mineral, found in all zones with the exception of intermediate zone II. It is found in the core as euhedral to subhedral crystals of cm. size, and is occasionally altered to muscovite. In the intermediate and wall zones microcline forms euhedral crystals or anhedral grains from medium to very coarse grain size. The microcline is always perthitic, with well developed grid-iron twinning. The colour varies from grey to brownish black to shades of red. In intermediate zones I and V the microcline is replaced by muscovite, quartz and minor amounts of rutile, xenotime, magnetite, apatite, and tourmaline. The nature of the replacement is problematic but the alteration appears to be concentrated along small



cracks. Åmli (1977) postulates that percolating solutions caused the alteration.

Anhedral masses of plagioclase are the dominant constituent in intermediate zones II and III. Plagioclase is also present in the outer intermediate zones and the wall and border zone. In intermediate zone IV it is graphically intergrown with quartz. In the other zones it is present in variable amounts as subhedral to anhedral masses. The plagioclase is characteristically sericitized or muscovitized. The degree of alteration is variable. In heavily muscovitized plagioclase occasional cavities are filled with calcite and rimmed with muscovite books up to 3 cm. across. The plagioclase is dominantly sodic oligoclase. Sericitization appears to increase the albite content. The composition of the plagioclase ranges from  $Ab_{82}$  to  $Ab_{96}$ . The albite twins show signs of stress, including bending and displacement.

Biotite is present in all zones with the exception of the core and intermediate zone II. In intermediate zone I it forms bent sheets of dm. size. In the other zones biotite is present as thin laths up to 2 cm. in length. It is occasionally weakly chloritized.

Muscovite is present in zones I, II, and III, as euhedral to subhedral books up to a few cm. across. It is a silvery green colour and is visibly zoned. The zoning is expressed as variations in the shades of green. The muscovite occurs as randomly oriented plates within feldspar, and as fine-grained oriented plates apparently replacing feldspar. Thin section examination of muscovitized, crumbly feldspar suggests that there has been at least two phases of muscovite development.

Pyrite, magnetite, rutile and prismatic black tourmaline occur in the core and in the inner intermediate zones in trace amounts





characteristically associated with microcline alteration. Tourmaline also occurs as inclusions in quartz. Magnetite occurs as both inclusions in quartz and as anhedral crystals in the wall and border zone.

$\beta$ -uranophane, uranophane, kasolite, uraninite, thorite, euxenite, allanite, zircon, and yttrotitanite are all intimately associated in intermediate zone III. The zircon occurs as an intergrowth with or an inclusion in euxenite and apatite. Allanite is the most abundant rare earth mineral and occurs as subhedral to anhedral cm. sized reddish brown masses. Only single specimens of uraninite and yttrotitanite were found in the pegmatite. Euxenite is found as euhedral to anhedral brown or black crystals up to a cm. in size. It is most abundant in intermediate zone III, but is also present in intermediate zone I and the wall zone. The colour change from black to brown is believed to be related to the degree of alteration (ie. the degree of leaching of U and Th)(Amli, 1977). In thin section, the euxenite is isotropic in character, which is typically indicative of metamict character. Uranophane,  $\beta$ -uranophane and kasolite are intimately associated with euxenite and probably formed through leaching (of euxenite) by percolating solutions. They form lemony-yellow films and pockets (probably pseudomorphous after euxenite).



## CHAPTER IV RUBIDIUM-STRONTIUM GEOCHRONOLOGY

### INTRODUCTION

The rubidium-strontium method of geochronology was used to date the formation of the Gloserheia granite pegmatite. This decay scheme was considered to be most suitable because of the abundance of rubidium in well distributed silicate mineral phases and because the half-life of rubidium is of the appropriate order of magnitude to date a (presumed) Precambrian body of igneous rock. The initial strontium isotope ratio was determined by the 'isochron' method. This ratio is regarded as important because it reflects the geochemical history and thus the source of the strontium, and as such is an important petrogenetic indicator.

Four mineral phases were available for Rb-Sr dating. Two of the mineral phases, biotite and microcline, were interpreted to be early-crystallizing on the basis of petrographic inspection. The nature of the plagioclase (sodic oligoclase) and muscovite was ambiguous, for both these minerals have extensively replaced primary feldspar, and muscovite books have encrusted crystals of quartz and feldspar. These relationships probably developed during the final stages (possibly the hydrothermal stage) of crystallization of the pegmatite, or during a subsequent period of metamorphism.

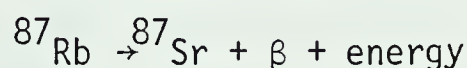
### Rubidium-Strontium Isotope Systematics

Although many geologists have some familiarity with geochronology, a brief summary of the basic principles of Rb-Sr isotope systematics is given here. The interested reader is referred to comprehensive reviews of the subject by Faure and Powell (1972) and Faure (1977).

Rubidium has one radioactive isotope of interest,  $^{87}\text{Rb}$ . This



'parent' nuclide disintegrates at a known rate according to the law of radioactive decay ( $N=N_0e^{-\lambda t}$ ) to form a stable strontium isotope 'daughter' according to the following reaction:



The abundance of  $^{87}\text{Sr}$  in a mineral is expressed by the equation:

$$^{87}\text{Sr} = ^{87}\text{Sr}_N + ^{87}\text{Rb}(e^{\lambda t}-1)$$

where ' $^{87}\text{Sr}_N$ ' is the number of atoms of this isotope incorporated into the same unit weight of this material at the time of its formation, ' $\lambda$ ' is the decay constant of (in this case)  $^{87}\text{Rb}$ , and 't' is the time elapsed in years since the mineral formed.

The 'date' becomes an 'age' when the mineral has remained isotopically closed, when the proper correction is made for the initial  $^{87}\text{Sr}/^{86}\text{Sr}$  ratio, and when the analytical results are accurate and representative of the material dated. An internal check of the satisfaction of these requirements is provided by dating the components of a rock (ie., the minerals), or dating a suite of cogenetic igneous rocks. If the dates are discordant, either an inappropriate correction was made for normal Sr or the system has not remained isotopically closed. Both of these possibilities may be pursued with the isochron method, which is based on the following precepts.

Cogenetic igneous rocks crystallizing from an isotopically homogeneous source over a relatively short time period should have the same initial  $^{87}\text{Sr}/^{86}\text{Sr}$  ratio. These phases should plot on a single straight line (or isochron) with coordinates of  $^{87}\text{Sr}/^{86}\text{Sr}$  (y) and  $^{87}\text{Rb}/^{86}\text{Sr}$  (x). The slope of the isochron is controlled by the age of the system, or in effect, the amount of radiogenic parent ( $^{87}\text{Rb}$ ) that has disintegrated through time. This relationship can be expressed





mathematically as  $m = e^{\lambda t} - 1$ ; where 'm' is the slope of the line, 't' is the time of formation of the system, and ' $\lambda$ ' is the decay constant of (in this case)  $^{87}\text{Rb}$ . The intercept of this line with the y axis is the value of the  $^{87}\text{Sr}/^{86}\text{Sr}$  ratio at the time of formation of the system, and represents the relative amount of  $^{87}\text{Sr}$  initially incorporated into the mineral lattice. With this method, the initial  $^{87}\text{Sr}$  ratio can be accurately determined. This initial ratio may be used as a petrogenetic indicator, because it is inherited from the source of the magma. Secondly, the slope of the line defines the age 't' at which that group of minerals or rocks last behaved as a closed system. For a group of minerals that time might not correspond to the time of crystallization of the rock, but rather to the last metamorphic event.

Metamorphic processes almost invariably cause readjustment of the chemical constituents of a rock, and this movement may result in recrystallization of existing minerals. Radiogenic Sr, because it imperfectly replaces  $^{87}\text{Rb}$  in a mineral lattice, is a mobile component and thermal events frequently result in isotopic rehomogenization. The mobility of Sr does not often extend to the whole rock scale, so while the minerals behave as open systems, the rock itself remains closed. The significance of this is that, if the Sr is completely rehomogenized, a mineral isochron will indicate the most recent episode of metamorphism, while an isochron based on the analysis of a comagmatic suite of (whole) rocks normally indicates the time of crystallization of that suite.

The interpretation of isochrons hinges upon the assumption of ideal, open system behavior on one scale and closed system behavior on the other. While closed systems can be demonstrated to exist down to the geological hand specimen scale, this is not always the case. This is dependent on



the mechanism of nuclide (or isotope) exchange. (Fletcher and Hofmann, 1974) and the scale of compositional heterogeneity (Hamilton, 1965). For minerals, complete isotopic re-equilibration seems reasonable for the case of complete melting, but it is more difficult to envisage for cases of minor recrystallization. If the data points can be fit to an isochron, one may safely presume that the basic requirements have been met. However, there are many cases where an isochron cannot be fit to the isotopic compositions of cogenetic samples (for example, this study). If the reason for this failure can be deduced, one may gain insight into the geological processes affecting the system.

One approach to the resolution of these difficulties has been field investigation of age discordancies controlled by one geological process. The classic example of this approach was reported by Hart (1964). The effect of the intrusion of the Eldora stock into the Precambrian in the Colorado Rockies was monitored by a detailed study of the isotopic response of the major mineral phases. The apparent age of a mineral could be correlated to its distance outward from the intrusive contact. Other such studies have been reported, but a great number of unknown parameters clearly affect the findings, and the conclusions drawn are correspondingly reduced to generalities. Moreover, many geological processes are not amenable to this type of study, either because a process may not result in a pronounced effect, or because subsequent processes have modified the physical and chemical state of the material, obscuring the initial effect.

To clarify some of the parameters, considerable laboratory study has been directed towards the diffusive processes that operate in a



geological system. Unfortunately laboratory conditions do not lend themselves to the study of high pressure and temperature kinetics or to the study of long-term mechanisms. Moreover, because so little is known about these processes, experiments must be so simplified and the variables so tightly controlled that it becomes difficult to reliably extrapolate the conclusions to natural systems. Still, valuable contributions have been made.

Heating experiments conducted on rock samples (eg. Baadsgaard and van Breemen, 1970; Hanson, 1971) have demonstrated closed system behavior on the scale of a hand specimen. These experiments have also shown that Rb, Sr, K, and Na concentrations shift in individual minerals in response to heating, and that Sr isotope composition has a tendency to homogenize. Muscovite and biotite have been found to lose Rb and  $^{87}\text{Sr}$ , and to gain normal Sr, while low Rb phases such as albite and apatite appear to gain  $^{87}\text{Sr}$  (Kesmarky, 1977). Brooks (1968) has demonstrated that the isotopes  $^{87}\text{Rb}$ ,  $^{86}\text{Sr}$  and  $^{87}\text{Sr}$  tended to "migrate" from potassium feldspar to fine-grained plagioclase alteration products.

Studies in rock systems have proved difficult to quantify, so attention has been directed towards single-mineral studies which are highly simplified and again further removed from natural systems. Hofmann (1969) and Foland (1972) considered the premise that radiogenic  $^{87}\text{Sr}$  is more mobile than common Sr and demonstrated that radiogenic  $^{87}\text{Sr}$  effectively behaves like common Sr - at least under hydrothermal experimental conditions. This was attributed to the mechanism of nuclide migration in mineral lattices.

Metasomatic processes are regarded in terms of reaction between rock-forming minerals and mobile aqueous solutes (Hofmann, 1972;





Korzhinskii, 1965, 1970). It has long been recognised that ion exchange has important effects on mineral Rb-Sr ages (Giletti, 1974) but it has been difficult to isolate the mechanisms. Many of the experiments have resulted in chemical alteration rather than diffusion (eg. Kulp and Bassett, 1961; Gerling and Ovchinnikova, 1962; Kulp and Engels, 1963); or in breakdown of the minerals due to instability at high temperatures (eg. Baadsgaard and van Breemen, 1970; Hanson, 1971). Hofmann and Giletti (1970) examined K and Na exchange between biotite and water, and concluded that K and Na exchange operated at equal rates; however Giletti (1974) and Foland (1974) dispute this and suggest instead that the mechanism of K and Na diffusion are independent of each other. Feldspars have proved especially difficult to study because of variable internal composition commonly expressed as perthite. Still, feldspars merit considerable attention because they are a sensitive indicator of metasomatic (K-Na) exchange activity (Robertson, 1959). Petrovic (1972) has considered the mechanism of ion exchange and Na and K diffusion in perthitic feldspars. Foland (1972) investigated alkali diffusion in orthoclase and commented on the experimental difficulties encountered in studies of Rb diffusivities. These studies are more concerned with mechanics than applications, but only the applications are of concern to most geologists. Still, it appears that the assumption of closed system behavior of the scale of hand-specimens and mineral scale open system behavior is generally not a problem, with the exception of alkali metasomatism. K and Na appear to readily exchange, and in all probability, Rb and Sr occupying the same cation lattice sites exchange along with them. The reaction rate appears to be enhanced by the apparently catalytic effect of an  $H_2O$  species (Foland, 1974). O'Neil



and Taylor (1967) have shown that under disequilibrium experimental conditions alkali ion exchange is additionally linked to oxygen isotope exchange.

In the Gloserheia pegmatite, metasomatic processes appear to have at least locally affected the feldspar phases, manifested by the turbid, heavily sericitized nature of the plagioclase and the development of replacement-type mesoperthite in the inner zones. In addition, carbonate and hematite are concentrated along fractures and the biotite is brittle and (weakly) chloritized. It seems reasonable that if cation exchange has occurred, the Rb-Sr ages would be affected, and could result in scatter of the data points on an isochron plot.

In summary, silicate mineral phases from the Gloserheia pegmatite were analysed by the Rb-Sr technique to determine the age of the pegmatite body, and to obtain mineral isotope data in the hopes of determining the factors that governed the emplacement of the pegmatite and the nature of the uranium mineralization.

### SAMPLES

In the Gloserheia pegmatite, four mineral phases were suitable for Rb-Sr dating. These were muscovite, biotite, plagioclase and microcline. These minerals were abundant and well distributed throughout the internal zones. Detailed sample descriptions are located in Appendix A.

Muscovite was sampled from the core zone, and the first and second intermediate zone. The core sample was composed of fresh books of muscovite up to cm. size partially encrusting the surface of a quartz crystal. In the intermediate zones, muscovite plates were enclosed by feldspar and formed crusts on unattached surfaces of the crystal. Some of the muscovite was parallel in orientation, suggesting that at least



portion formed by replacement.

Biotite was sampled from the first four intermediate zones. The samples from the first two intermediate zones were large books of gently crenulated biotite, weakly chloritized and hematite stained on the surfaces. Biotite in the single sample from the third intermediate zone was present as hexagonal cm. sized books with attached rare earth bearing minerals (ie. allanite, euxenite). Biotite from the fourth intermediate zone occurred as variably chloritized laths interstitial to coarse-grained feldspar.

During preparation for sample analysis of muscovite and biotite, altered material was physically removed where possible, and uniform fractions were separated on the basis of magnetic properties and specific gravities.

Both sodic and potassic feldspar were present. Microcline was characteristically perthitic, and exhibited pronounced grid-iron twinning. It was generally fresh in character, but incipient local alteration was concentrated along fractures and in perthite strings. Microcline was found in all zones with the exception of intermediate zone II. In the outermost zones microcline occurred in a graphic-textured intergrowth with sodic oligoclase and/or quartz while in the inner zones it occurred as large blocky crystals. A small amount of untwinned potassic feldspar (orthoclase ?) was present in the outer zones, and appeared to be replacing oligoclase. It was altered to variable degrees. Oligoclase was present in every zone with the exception of the core zone. The composition ranged from  $Ab_{82}$  to  $Ab_{96}$  and was apparently related to degree of alteration. Oligoclase in the outer zones appeared to be primary, but in the inner zones it was





characteristically heavily muscovitized and formed a replacement mesoperthite in samples IZ1-4, IZ2-2, -3 and -6.

Perthites and alteration products were separated with the use of heavy liquids. In cases where two distinct gravity fractions were present, and the specific gravity of these fractions was similar, both fractions were retained for analysis. Otherwise the relatively dense, homogeneous fraction was selected.

#### ANALYTICAL

The rock samples were crushed and the mineral phases were separated and purified as described in Appendix B. Chemical separations were performed as described in Appendix C, in preparation for isotopic analysis on a mass spectrometer. In brief, each mineral separate was spiked with a mixed solution of  $^{87}\text{Rb}$  and  $^{84}\text{Sr}$ , and then equilibrated by decomposition in HF and  $\text{HNO}_3$ . Rb was separated from Sr using the barium coprecipitation method. The Sr was further purified by elution through an ion exchange column, while the Rb was precipitated as a perchlorate. Samples were loaded on outgassed rhenium double filaments.

The spikes used were prepared and calibrated by Dr. H. Baadsgaard. The spikes contained  $\sim 2 \text{ ug/g } ^{84}\text{Sr}$  and either  $\sim 200$  or  $\sim 5.5 \text{ ug/g } ^{87}\text{Rb}$  per gram of solution. Choice of spike was based on approximate Rb and Sr concentrations determined by XRF analysis. Several blank determinations on the analytical procedure were run by Dr. Baadsgaard and the author during the time interval of laboratory work. The blanks were found to contain about 1 nanogram of Sr and 2.5 nanograms of Rb.

The isotopic composition of the samples was determined on a 30 cm. radius of curvature  $90^\circ$  sector single focussing solid source mass



spectrometer, the Aldermaston Micromass 30. The spectrometer was equipped with peak-switching facilities, and an on-line Hewlett-Packard 9825A minicomputer. The isotope masses were measured by switching between preset magnet current positions and recording the digital voltmeter output. The Sr isotopic data was corrected for fractionation by normalizing the  $^{86}\text{Sr}/^{88}\text{Sr}$  (atomic) ratio to 0.1194. Analysis of Sr and Rb in a standard reference material, NBS Feldspar 607, gave the following results:

total Sr = 67.4 ppm; total Rb = 520.6 ppm;  $^{87}\text{Sr}/^{86}\text{Sr} = 1.2015 \pm 0.0004$  which compared favourably to the certificate of analysis values (total Sr =  $65.5 \pm 0.3$  ppm; total Rb =  $524 \pm 1$  ppm;  $^{87}\text{Sr}/^{86}\text{Sr} = 1.20039 \pm 0.00002$ ). Analytical precision is estimated to be about  $\pm 0.5\%$  of the total Sr content. Rubidium isotopic ratios cannot be corrected for fractionation, so Rb determinations may only be accurate to  $\pm 1$  or  $2\%$ . Repeats of samples are included in Table 2. The variation observed in the Sr ratios and  $^{87}\text{Rb}/^{86}\text{Sr}$  ratios in repeat samples is attributed to sample inhomogeneity related to the coarse grain size.

## RESULTS

Fortynine mineral separates from the Gloserheia pegmatite were analysed for their Rb and Sr isotopic compositions. Analytical data for the samples is presented in Table 2. The results are graphically presented on conventional Nicolaysen isochron diagrams in Figures 4 and 5. A reference isochron fitted to eleven fresh potassium feldspars and three fresh oligoclase samples defines an age of  $1009 \pm 6$  m.y. (standard deviation given as  $2\sigma$ ) with an initial ratio of  $0.7135 \pm 0.0008$  (at  $2\sigma$ ) using a  $\lambda$  value for  $^{87}\text{Rb}$  of  $1.42 \times 10^{-11} \text{ yrs.}^{-1}$  (Steiger and Jager, 1977). The isochron has a mean square weight of deviates (MSWD) of 9.1, which is



TABLE 2. Rb/Sr analytical data for minerals from the Gloserheia pegmatite.

Sample Number		$^{86}\text{Sr}$ (ppm)	$^{87}\text{Rb}$ (ppm)	$^{87}\text{Rb}/^{86}\text{Sr}$ atomic ratio	$^{87}\text{Sr}/^{86}\text{Sr}$ atomic ratio
Potassium feldspar					
C-2	*	9.4773	146.49	15.279	0.9362
CI-1	*	7.7928	122.98	15.600	0.9398
CI-4	*	7.0063	142.42	19.923	1.0021
IZ1-5	*	6.5390	143.63	21.712	1.0292
IZ1-11	*	7.4363	130.52	17.349	0.9612
IZ2-4		3.3081	15.376	4.594	0.7845
IZ5-1	*	5.3369	93.329	17.286	0.9601
WZ-1		11.8079	12.980	1.0866	0.7262
Plagioclase					
IZ1-4		3.0078	0.5015	0.1648	0.7223
IZ2-2		3.2183	0.2210	0.0679	0.7182
IZ2-3		2.2707	0.2478	0.1079	0.7196
IZ2-6		1.0935	0.6484	0.5862	0.7275
IZ2-7		5.7252	3.7235	0.6429	0.7185
IZ2-8		2.4478	0.7001	0.2348	0.7208
IZ3-2		6.7749	6.1227	0.8933	0.7257
IZ3-3		6.5803	4.7036	0.7066	0.7230

\* relatively unaltered mineral sample used to calculate the best isochron.





TABLE 2. Continued.

Sample Number		$^{86}\text{Sr}$ (ppm)	$^{87}\text{Rb}$ (ppm)	$^{87}\text{Rb}/^{86}\text{Sr}$ atomic ratio	$^{87}\text{Sr}/^{86}\text{Sr}$ atomic ratio
Feldspars. Heavy liquid separated pairs.					
IZ1-8	+ *	6.5809	13.864	2.8025	0.7435
IZ1-8	-	5.2973	3.6910	0.6887	0.7234
IZ1-10	+	2.7084	82.931	30.267	1.1078
IZ1-10	-	2.6345	54.032	20.273	0.9783
IZ4-1	+ *	4.6603	92.343	19.587	0.9994
IZ4-1	+	4.7511	90.860	18.904	0.9894
IZ4-1	- *	2.8429	1.3779	0.4791	0.7208
IZ4-1	- *	2.8835	1.6041	0.5499	0.7210
IZ4-2	+ *	4.6080	33.423	7.1667	0.8164
IZ4-2	- *	3.1175	2.6887	0.8525	0.7264
IZ5-2	+	3.5973	97.174	26.702	1.0857
IZ5-2	- *	2.2128	29.581	13.214	0.9018
IZ5-2	- *	0.2108	2.3943	11.225	0.8745
BZ-1	+	6.3712	125.73	19.507	1.0009
BZ-1	-	10.971	9.6044	0.8654	0.7241

\* - relatively unaltered mineral sample used to calculate the best isochron.

+ mineral separate with lighter specific gravity.

- mineral separate with heavier specific gravity.



TABLE 2. Continued.

Sample Number	$^{86}\text{Sr}$ (ppm)	$^{87}\text{Rb}$ (ppm)	$^{87}\text{Rb}/^{86}\text{Sr}$ atomic ratio	$^{87}\text{Sr}/^{86}\text{Sr}$ atomic ratio
Muscovite				
C-1	0.9809	121.87	122.80	2.2682
IZ1-4	0.9367	98.847	104.32	2.1772
IZ1-10	0.7529	104.34	136.99	2.6130
IZ2-1	0.8984	130.18	143.23	2.8307
IZ2-1	0.8815	130.77	146.64	2.8600
IZ2-2	1.0781	102.57	94.049	2.0042
IZ2-3	0.6547	55.734	84.146	1.9272
IZ2-6	0.7812	92.769	117.38	2.3374
IZ2-8	0.8739	104.66	118.37	2.4030
Biotite				
CI-1	0.5149	405.46	778.32	10.483
CI-2	0.3152	339.61	1253.4	18.112
IZ1-3	0.6927	448.63	640.16	8.334
IZ1-11	0.3056	442.68	1431.9	18.838
IZ2-5	0.2808	409.06	1440.2	19.460
IZ3-3	2.3002	69.439	29.841	1.0067
IZ3-3	2.1926	66.545	30.001	1.0130
IZ4-1	0.4651	454.05	965.08	13.484
IZ4-2	0.2908	496.56	1688.8	22.372
Apatite (unspiked)				0.7125



FIGURE 4. Plot of  $^{87}\text{Sr}/^{86}\text{Sr}$  ratios versus  $^{87}\text{Rb}/^{86}\text{Sr}$  ratios for feldspars from the Gloserheia pegmatite.

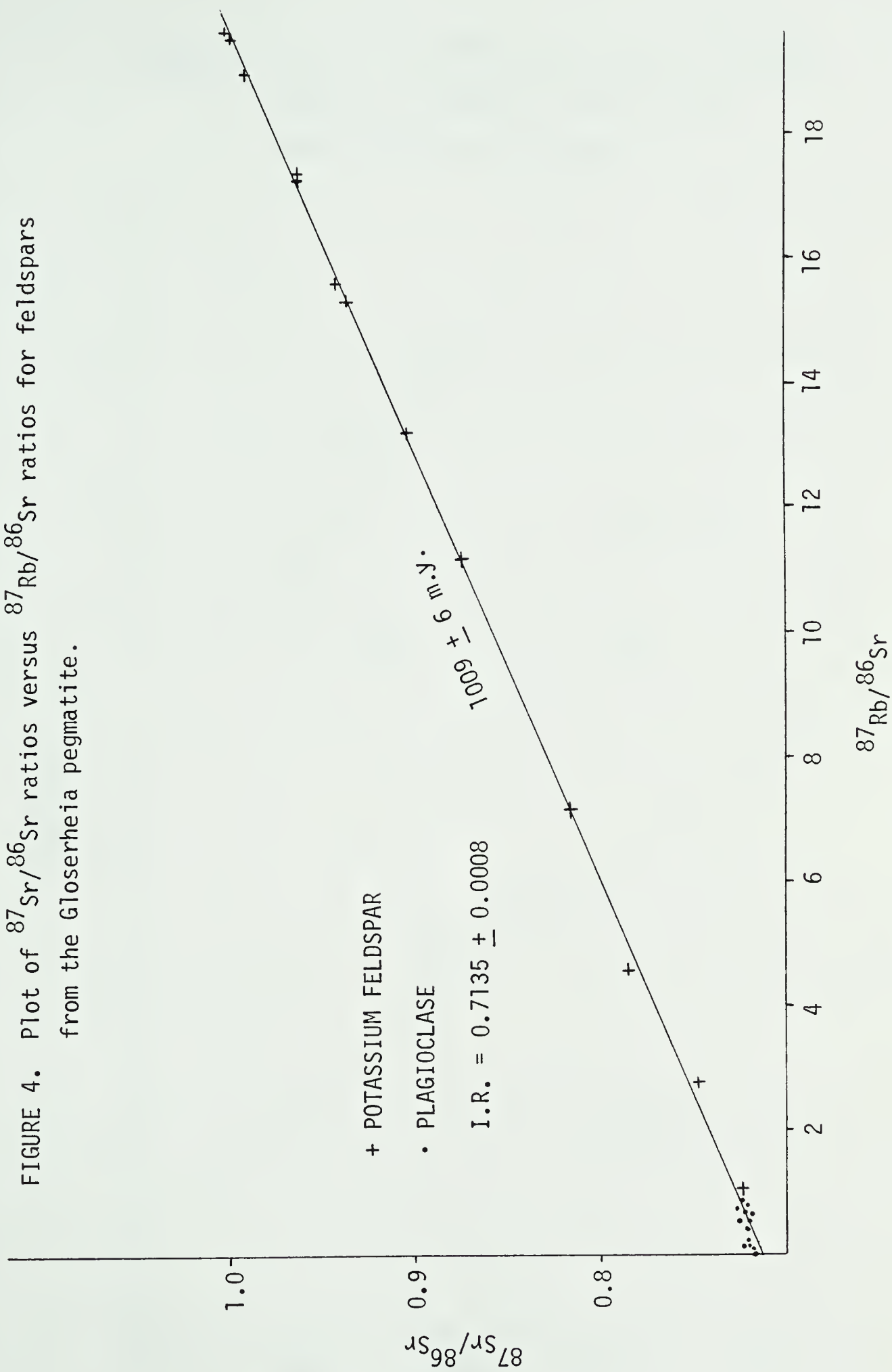
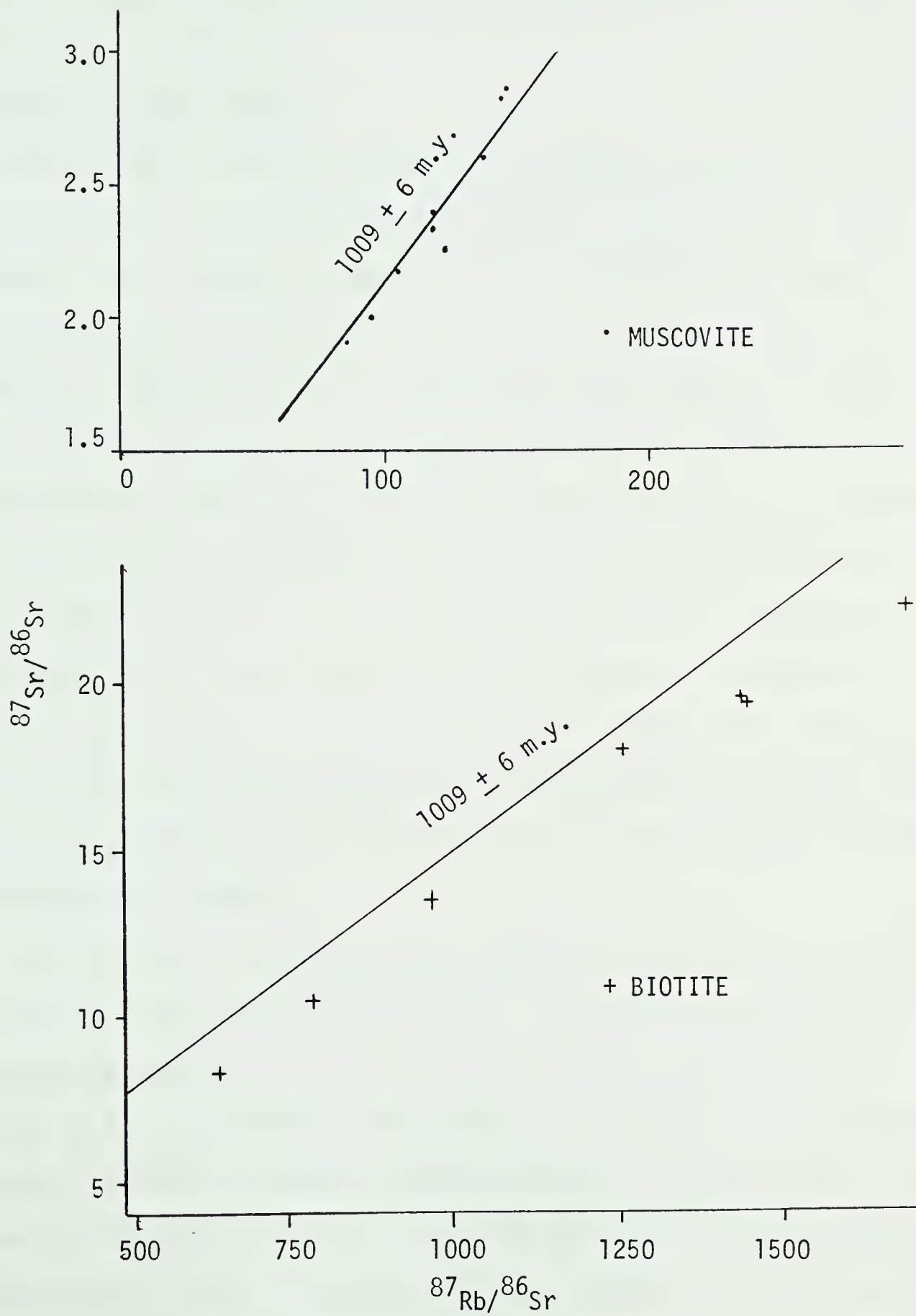






FIGURE 5. Plot of  $^{87}\text{Sr}/^{86}\text{Sr}$  ratios versus  $^{87}\text{Rb}/^{86}\text{Sr}$  ratios for muscovites and biotites from the Gloserheia pegmatite.





in excess of the permitted deviation for experimental error only. (The MSWD is a quantity analogous to the residual variance in a simple treatment, and has a  $\chi^2$  distribution and an expected value of 1 if the scatter of points in the isochron is due to experimental error alone. McIntyre et al, 1966).

### DISCUSSION AND CONCLUSIONS

When the Rb-Sr data is plotted on a Nicolaysen diagram, it is apparent that a 'scatterchron' -not an isochron- (Brooks et al, 1972) is formed. In an isochron diagram, values of  $^{87}\text{Sr}/^{86}\text{Sr}$  determined for a suite of cogenetic mineral or rock samples are plotted versus their respective  $^{87}\text{Rb}/^{86}\text{Sr}$  values. If the samples were cogenetic, if they were initially homogeneous with respect to  $^{87}\text{Sr}/^{86}\text{Sr}$  composition, and if no subsequent modification of Rb or Sr composition occurred, a linear relationship should be defined by the data points, and a line joining them is termed an isochron. A small degree of scatter is permitted within the limits of experimental error. The data, as presented in Figures 4 and 5, clearly do not form a precise linear array. However, techniques of data reduction do permit a statistically significant line to be constructed connecting the data points from the fourteen relatively unaltered mineral samples.

This isochron is based on eleven samples of perthitic potassium feldspar and three samples of oligoclase. The potassium feldspar was predominantly perthitic microcline, with only minor alteration that appeared to be concentrated in fine strings of more sodic (?) composition. Untwinned, relatively potassic feldspar (presumed orthoclase) was present in intermediate zone V. This same phase was present elsewhere in the outermost zones but was moderately kaolinized, and its isotopic



composition does not fit the reference isochron. Sodic oligoclase from intermediate zone IV is the only plagioclase to fit the reference isochron. The plagioclase in this zone showed minor sericitization compared to plagioclase samples in other zones.

The (potassic or sodic) composition of the feldspar mineral separates was assessed on the basis of thin section examination coupled with the Rb/Sr ratio. Where feldspars of two compositions were present in a rock sample, the phases were separated on the basis of specific gravity variation. Inspection of the distribution of data with respect to the potassium feldspar isochron suggests that this separation either was not always successful, or alternatively that some of the variation in specific gravity was due to the presence of fine-grained alteration products that may have soaked up excess  $^{87}\text{Sr}_r$  and/or  $^{87}\text{Rb}$  as suggested by Brooks (1968).

In thin section, the feldspar samples that fit the reference line were relatively unaltered in comparison to the feldspar samples that scatter above and below. This suggests that some event has resulted in local variable alteration after the time of isotopic closure of the (unaltered) feldspar samples. The samples that plot above the reference line were characteristically very heavily muscovitized, and had very low  $^{86}\text{Sr}$  and  $^{87}\text{Rb}$  contents. These samples may either have gained Sr or lost Rb, or both. With such low quantities of both nuclides it is difficult to assess the likelihood of either event. The isotope composition of feldspar samples that plot below the reference line had greater proportions of  $^{87}\text{Rb}$  and were only moderately sericitized. These samples either lost  $^{87}\text{Sr}_r$  or gained  $\text{Sr}_N$  and/or Rb. It seems unlikely that





oligoclase would have gained Rb, unless the Rb concentrated in the sericitic alteration and this fraction was incompletely removed during sample purification. Alternatively,  $^{87}\text{Sr}_r$  could have been lost and  $\text{Sr}_N$  gained through Sr isotopic homogenization during metamorphism.

The same event that has variably affected the feldspars at less than 1009 m.y. has also apparently disturbed the pegmatite's micas. The isotope compositions of the samples of biotite and muscovite dominantly plot below the potassium feldspar reference line in the region of  $^{87}\text{Sr}$  loss or Rb and  $\text{Sr}_N$  gain. Biotite appears to have been more susceptible to isotope redistribution than muscovite. Both micas had very high  $^{87}\text{Sr}/^{86}\text{Sr}$  ratios, with biotite more enriched in nature than muscovite, so it seems unlikely that biotite would have (proportionally) gained much  $^{87}\text{Rb}$  (for lack of a source). Sr only poorly replaces Rb in the mica lattice, and because of this the micas, and biotite in particular, are known for their sensitivity to Sr isotopic readjustment during metamorphism. (Baadsgaard, 1965).

The observed distribution of isotopes in the mineral phases of the Glosseheia pegmatite is in accord with the experimental findings of Hanson (1971), Baadsgaard and van Breemen (1970), and Kesmarky (1977). In these experiments, rock samples were heated in air and then examined for cation and isotope redistribution. Alkali ion exchange was found to occur between the K and Na minerals. Rb and Sr isotope compositions were found to shift in the direction of isotope rehomogenization. Biotite was found to lose  $^{87}\text{Rb}$  and  $^{87}\text{Sr}_r$  more readily than muscovite, while both micas gained  $\text{Sr}_N$ . Potassium feldspar was found to show only minor shift in composition, losing small quantities of Rb and  $^{87}\text{Sr}_r$ ,



while in comparison, plagioclase changed slightly but erratically. Potassium feldspar was concluded to be the most reliable mineral phase for dating (under such conditions).

In the Gloserheia pegmatite, some event has resulted in partial isotope and cation (Na-K) exchange. The visibly altered nature of the biotite, the brittle character of both micas, and the late-crystallized or secondary nature of the muscovite suggests that open system behavior, at least on a mineral scale, has occurred. Although the physical conditions that would facilitate ion exchange exist during the late hydrothermal stage of crystallization of complex pegmatites, exchange during this stage is regarded as unlikely. The micas have apparently lost a proportion of radiogenic Sr, and because of the long half-life of Rb, the Sr is not 'instantaneously' (geologically speaking!) generated. Thus, the event must have happened subsequent to the completion of crystallization (ie. < 1009 m.y.).

This event is presumed to be minor in scale, for it was of insufficient in magnitude to cause isotopic rehomogenization. Complete isotope exchange does not occur even at very high (greater than 1000°C) temperatures if conditions are 'dry'. (for example the experiments of Baadsgaard and van Breemen, 1970). It seems highly unlikely that any natural system would be dry, and in the Gloserheia pegmatite there is petrographic evidence to suggest that an aqueous phase was present after the time of crystallization of the various mineral phases. Aqueous phases are well known to exert a pronounced catalytic effect on the rate of recrystallization and ion exchange, permitting equilibrium exchange conditions to be met at much lower temperatures. Under aqueous conditions and at moderate temperatures, isotopic exchange would be



expected to be complete. Because this homogenization is not observed, it is reasonable to conclude that the event must only have been minor, disturbing the more sensitive mineral phases but leaving the potassium feldspar relatively unchanged. The date of  $1009 \pm 6$  m.y. derived from the isochron based on unaltered and dominantly potassic feldspars may be regarded as the time at which those minerals last behaved as a closed system and began to accumulate  $^{87}\text{Sr}_r$  from the decay of  $^{87}\text{Rb}$ . This date falls within the range (albeit towards the lower end) of isotope ages published for the Sveco-Norwegian event in the Bamble sector of the Baltic Shield.

The 'initial'  $^{87}\text{Sr}/^{86}\text{Sr}$  ratio of  $0.7135 \pm 0.0008$  obtained from the potassium feldspar isochron and the  $^{87}\text{Sr}/^{86}\text{Sr}$  ratio of  $0.7125 \pm 0.00002$  obtained from one analysis of apatite may be used as a petrogenetic indicator. The application of variations of the  $^{87}\text{Sr}/^{86}\text{Sr}$  initial ratio has become a relatively well established technique. Material (presumably) derived from the mantle, such as oceanic basalt, has a relatively low initial Sr isotope ratio in the range of 0.702-0.706 (Faure and Powell, 1972), while continental crustal material is relatively enriched in  $^{87}\text{Sr}$ . This variation permits identification of Sr present through reworking of or contamination by crustal material of sialic composition.

In order to deduce the magmatic source of the Gloserheia pegmatite, two models must be evaluated: (i) the 'initial' ratio of the unaltered feldspars represents the original magmatic  $^{87}\text{Sr}/^{86}\text{Sr}$  composition of the magma; or (ii) the  $^{87}\text{Sr}/^{86}\text{Sr}$  ratio of the unaltered feldspars represents the homogenized Sr isotope ratio at the time that the feldspars last behaved as a closed system, and if there has been a metamorphic episode





this ratio is by definition not the initial ratio at the time of formation of the pegmatite. In this case, the apatite Sr ratio may provide the upper limit for the true value although it should be noted that the error ranges of the two values just overlap. The second hypothesis is preferred because of independent evidence of metamorphic activity; ie. the U-Pb date for crystallization of U-bearing minerals was 1055 m.y. If the second hypothesis is adopted, it becomes necessary to consider the initial Sr ratio of the pegmatite at about 1055 m.y. This may be approximately calculated by assuming that the dominant Rb-bearing mineral phase in the pegmatite was feldspar, and selecting a typical  $^{87}\text{Rb}/^{86}\text{Sr}$  ratio. Because the bulk composition of the pegmatite is unknown, a range should be considered of about 6-12. In 50 m.y. the  $^{87}\text{Sr}/^{86}\text{Sr}$  ratio would have increased by about 0.004 to 0.008, so the initial ratio of the minerals at 1055 m.y. would have been between 0.705 and 0.709. The lower initial ratio is typical of juvenile mantle-derived igneous material. Ratios in this range are also typical of the ranges observed by Field and Raheim (1979) for high grade metamorphic amphibolites in the Arendal region, which may through anatexis have provided the source of the pegmatitic magma. In order to choose between these two models, independent evidence is necessary, and is provided by petrographic examination and oxygen isotope composition. These factors will be considered together in the final chapter.

In conclusion, an isochron based on fourteen unaltered feldspar samples suggests a crystallization date of  $1009 \pm 6$  m.y., which may be the time of crystallization of the pegmatite, or the time of a subsequent metamorphic event. Scatter of the isotopic ratios of altered feldspar, biotite, and muscovite suggest that the subsequent small-scale open



system activity occurred after that time, affecting only the mineral phases more sensitive to isotopic readjustment. The nature of the 'initial' Sr isotope ratio is ambiguous, for the ratio may not be in the strict sense initial. On the basis of the Sr isotopic data alone, it is not possible to more than speculate on the original source of the pegmatite magma.



## CHAPTER V URANIUM-LEAD GEOCHRONOLOGY

### INTRODUCTION

The uranium-lead method of geochronology was implemented to provide additional information about the geochronology of the Gloserheia granite pegmatite, since uranium-bearing mineral phases are present in the pegmatite. The pegmatite is believed to be Precambrian in age and because of the long half-life of uranium, the U-Pb system is an appropriate method

In this study the U-Pb system was used as a check on the Rb-Sr age. If the pegmatite crystallized under restricted-system conditions, and if the system and its component minerals remained closed after formation, the Rb-Sr and U-Pb 'clocks' should yield the same radiometric date, corresponding to the age of crystallization of the pegmatite. If, however, the pegmatite suffered subsequent metamorphism, one or both systems should show departure from ideal behavior. Because the geochemical behavior of the elements involved varies considerably, the U-Pb pair would be expected to respond differently than the Rb-Sr pair to tectonism or hydrothermal activity. This is due at least in part to the different mineral types involved (ie. silicates (Rb-Sr) versus complex oxides and phosphates (U-Pb)).

Two mineral phases were available for U-Pb dating. Euxenite, a complex REE-bearing oxide, occurred as well-formed crystals scattered in bands in coarse-grained feldspathic rocks. Xenotime occurred as microcrystalline inclusions in apatite crystals. These minerals were analysed to determine their radiometric age, which (according to Jahns and Burnham's 1969 model) should correspond to the age of the pegmatite.





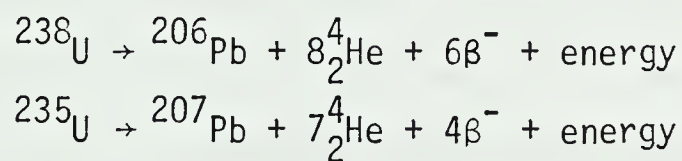
Alternatively, the uranium mineralization may have formed subsequent to crystallization of the pegmatite, through the action of uranium-bearing hydrothermal fluids along channelways. In this case the U-Pb age might post-date the Rb-Sr age.

In summary, the U-Pb geochronometric method was expected to indicate the age of the uranium mineralization of the pegmatite (which may or may not conform with the Rb-Sr mineral age obtained by the isochron method) and to reveal if a subsequent metamorphic pulse occurred that was sufficient in magnitude to cause readjustment of the isotope systematics.

### Uranium-Lead Isotope Systematics

Although many geologists have some familiarity with radiometric dating, a brief review of the basic principles of U-Pb geochronology is given here. The interested reader is referred to more detailed reviews by Baadsgaard (1965), Hamilton (1965), Hamilton and Farquhar (1968), and Faure (1977).

Uranium-bearing minerals have two radioactive isotopes of interest:  $^{238}\text{U}$  and  $^{235}\text{U}$ . These parent nuclides disintegrate at known rates according to the law of radioactive decay ( $N = N_0 e^{-\lambda t}$ ) to form stable lead isotope daughters according to the following reactions:



The isotopic composition of lead in these minerals is expressed by the following equations:

$$\begin{aligned} ^{206}\text{Pb} &= ^{206}\text{Pb}_N + ^{238}\text{U}(e^{\lambda_{238}t} - 1) \\ ^{207}\text{Pb} &= ^{207}\text{Pb}_N + ^{235}\text{U}(e^{\lambda_{235}t} - 1) \end{aligned}$$

where ' $\text{Pb}_N$ ' is the number of atoms of that isotope incorporated into the



same unit weight of this mineral at its time of formation; 't' is the time elapsed in years since the formation of the mineral, and 'λ' is the decay constant. These equations may be solved for 't'. The two equations may be combined to result in a third age equation:

$$\frac{{}^{207}\text{Pb}}{{}^{206}\text{Pb}} = \frac{{}^{207}\text{Pb}_N + {}^{235}\text{U}(e^{\lambda_{235}t_{207}} - 1)}{{}^{206}\text{Pb}_N + {}^{238}\text{U}(e^{\lambda_{238}t_{206}} - 1)}$$

Because the isotopic ratio of natural uranium is known ( ${}^{235}\text{U}/{}^{238}\text{U} = 137.88$ ) and is assumed to have remained constant over geologic time, this value may be substituted in the above equation and a 207/206 date may be calculated without determining the amount of the uranium.

Compatible dates may be obtained from these equations if a U-Pb bearing mineral has remained closed after formation, ie. if no U or Pb has been gained or lost, and if the appropriate correction is made for contaminant or 'common' lead incorporated into the mineral lattice at the time of formation. Wetherill (1956) devised a 'concordia' diagram, a plot of  ${}^{206}\text{Pb}/{}^{238}\text{U}$  versus  ${}^{207}\text{Pb}/{}^{235}\text{U}$ , where the locus of the points for which  $t_{207} = t_{206}$  form a curve. This has found wide application in geochronology.

Minerals frequently depart from ideal (ie. closed system) behavior, resulting in incompatible or discordant dates. The most common pattern of age discordancy, characteristic of zircons but also found in other minerals, is  $t_{206} < t_{207} < t_{207/206}$ . Reversed sequences are sometimes found. These patterns are attributed to either lead or uranium loss. If these U-Pb ratios are plotted on a concordia diagram they tend to lie on a chord cutting the concordia at two points. Wetherill (1956) proposed that the upper intercept represents the 'true' age of the system, while the lower intercept may mark the time of an episode of lead loss. This



lower age is regarded as meaningful if independent geochronological data is supportive.

There are, however, alternate explanations for discordant U-Pb ages. Nicolaysen (1957) and Tilton (1960) suggested that a similar pattern results from the continuous diffusion of radiogenic lead. Diffusion is proposed to occur at a rate determined by a constant diffusion coefficient, the effective radius, and the concentration gradient of the mineral. When diffusion occurs, the lower intercept of the discordia does not exist. Wasserburg (1963) expanded slightly on this model by proposing that the diffusion coefficient is a time-dependent function related to radiation damage of a crystal lattice by uranium decay. The diffusion trajectory is very similar to that in Tilton's model. Wetherill (1963) considered both uranium and lead diffusion.

Other interpretations include loss of intermediate nuclides from the uranium-decay series (Holmes, 1955; Kulp, 1955; Gilletti and Kulp, 1955), a possible but unpopular hypothesis (Catanzaro, 1968); and leaching of uranium and lead by water introduced through microcapillary channels created by radiation damage (the dilatancy model of Goldich and Mudrey, 1972).

It is widely accepted that both episodic and continuous diffusion processes are responsible for discordant ages. Frequently, however, the lower intercept of a discordia is ambiguous in meaning, and it is difficult to judge if diffusion processes or a metamorphic pulse is responsible for the age patterns. Independent geologic evidence is essential to make a proper judgement.

## SAMPLES

In the Gloserheia pegmatite, there are numerous mineral phases





suitable for dating by the U-Pb method. These include zircon, allanite, uraninite, sphene, euxenite, and xenotime. Several uranium secondary minerals were also present. However, only two of the minerals, euxenite and xenotime, were available in the collected sample suite.

Xenotime was present in the pegmatite as microcrystalline inclusions in apatite. A single sample of xenotime ( $\text{YPO}_4$ ), from the first intermediate zone, was provided. The sample was obtained by acid dissolution of an apatite crystal (Dr. W. Griffin, personal communication). Åmli (1975) postulated that the xenotime formed late, through exsolution in the apatite, probably in conjunction with metasomatic or hydrothermal activity.

The euxenite  $((\text{Y,Er,Ce,La,U})(\text{Nb,Ti,Ta})_2(\text{O,OH})_6)$  is described by Åmli (1975) as occurring only in the third intermediate zone. However, Dr. Griffin provided euxenite-bearing samples from the wall zone and the first and third intermediate zones. Respectively 1, 1, and 3 samples were chosen from these zones for analysis. The crystals were euhedral to subhedral tabular, and ranged from brown to black in colour. Discrete euxenite crystals ranged up to 0.5 cm. in size. In hand specimen and in thin section, the euxenite appeared to be concentrated along fracture bands interstitial to large crystals of feldspar. In thin section the euxenite is intimately associated with minor amounts of muscovite, carbonate, hematite and uranium secondary minerals interconnected along fractures. The isotropic nature of the euxenite in thin section suggests metamict, altered character, as does Åmli's (1977) X-ray diffraction and specific gravity data. Moreover, pockets of uranium secondary minerals such as  $\beta$ -uranophane, uranophane and kasolite are either associated with or pseudomorphous after euxenite. Associated



plagioclase is strongly sericitized and iron-stained. Åmli (1977) suggests that the uranium secondary minerals were formed from elements leached out of euxenite.

Euxenite and xenotime are not common minerals. Most of the known occurrences are in REE-bearing pegmatites. Consequently there is a paucity of information in the literature regarding their isotopic behavior. Kulp and Ecklemann (1957) briefly discuss the behavior of these two minerals in a review of discordant U-Pb ages and mineral type. Generally euxenite  $^{207}\text{Pb}/^{206}\text{Pb}$  ages are regarded as reliable but radiogenic lead is readily susceptible to leaching so the  $^{206}\text{Pb}/^{238}\text{U}$  and  $^{207}\text{Pb}/^{235}\text{U}$  ages are often strongly discordant in the characteristic pattern  $t_{206/238} < t_{207/235} < t_{207/206}$ . Xenotime tends to show the reverse age pattern.  $^{206}\text{Pb}$  is also lost. According to Mitchell (1973), metamict phosphates (including xenotime) are only rarely found. Euxenite, on the other hand, becomes typically metamict and typically contains large amounts of nonessential water in its structure. Goldschmidt (1924) suggested that a necessary condition for metamictization is that the structure contains ions readily susceptible to the changes in the state of ionization, especially the ions of the rare earths. It seems likely, then, that the tetravalent  $\text{U}^{+4}$  form in euxenite would be readily oxidized to the highly mobile hexavalent  $\text{U}^{+6}$  (Grandstaff, 1976), and that the euxenite would be susceptible to hydrothermal activity with exchange or loss of the radiogenic parents and daughters.

#### ANALYTICAL

The rock samples were crushed, and the mineral samples were separated and purified (as described in Appendix C) in preparation for



decomposition and isotopic analysis on a mass spectrometer. Briefly, each mineral separate was decomposed in HF and HNO<sub>3</sub>. Half the solution was spiked with <sup>235</sup>U and <sup>208</sup>Pb for isotope dilution determination of quantity. The remainder was used for Pb isotope ratio measurement. Uranium was separated from lead using the barium coprecipitation method and then both elements were purified by elution through ion exchange columns. The samples were loaded on outgassed rhenium double filaments.

The spikes were prepared and calibrated by Dr. H. Baadsgaard. The <sup>235</sup>U spike was composed of 9.7271 ug. <sup>235</sup>U and 0.0127 ug. <sup>238</sup>U per gram of solution. The lead spike was composed of 5.0183 ug. <sup>208</sup>Pb, 0.00251 ug. <sup>207</sup>Pb, and 0.01097 ug. <sup>206</sup>Pb per gram of solution. Blank determinations on the analytical procedure were run by Dr. Baadsgaard during this time period. The blanks contained less than one nanogram of uranium and a maximum of 3.8 nanograms of lead. The blank lead contamination was corrected out along with common lead during computations.

The isotopic composition of the samples was determined on a 30 cm. radius of curvature 90° sector single focussing solid source mass spectrometer, the Aldermaston Micromass-30 (Vacuum Generator). The spectrometer was equipped with peak switching facilities, and an on-line Hewlett-Packard 9825A minicomputer. The isotope masses were measured by switching between preset magnet current positions and recording the digital voltmeter output. The measurement precision of <sup>207</sup>Pb/<sup>206</sup>Pb and <sup>208</sup>Pb/<sup>206</sup>Pb was  $\leq 0.1\%$ . The <sup>206</sup>Pb/<sup>204</sup>Pb measurement precision of  $\pm 2\%$  was acceptable because of the minor common lead correction necessary. Measurement precision of <sup>238</sup>U/<sup>235</sup>U was about  $\pm 0.1\%$ .





## RESULTS

Analytical results and the ages and isotopic ratios used for plotting on a concordia diagram are presented in, respectively, Tables 3 and 4. Ages and ratios were calculated by an APL computer program written by Dr. H. Baadsgaard. The following constants, adopted internationally in the 1976 'Convention on the Use and Decay of Geo- and Cosmochronology' (Steiger and Jager, 1977), were determined by Jaffey et al (1971).

$$\begin{aligned} {}^{238}\text{U}/{}^{235}\text{U} &= 137.88 \text{ (atomic ratio, NBS value)} \\ \lambda_{\text{U}^{238}} &= 1.5513 \times 10^{-10} \text{ yr.}^{-1} \\ \lambda_{\text{U}^{235}} &= 9.8485 \times 10^{-10} \text{ yr.}^{-1} \end{aligned}$$

The measured isotopic ratios were corrected for nonradiogenic lead based on the composition of lead in a feldspar of equivalent model lead age ( ${}^{204}\text{Pb}:{}^{206}\text{Pb}:{}^{207}\text{Pb}:{}^{208}\text{Pb} = 1:16.04:15.24:37.11$ ) at  $\mu = 9.0$ ,  $T_0 = 4.56 \times 10^9$  yrs. No mass discrimination correction for the lead isotopes was necessary. The samples had large 206/204 ratios (ie. they had a high U content and little contaminant lead) so the error introduced in the correction for nonradiogenic lead was quite small.

The discordia was fit to the seven data points (6 euxenite samples, 1 xenotime sample) with the aid of an APL program written by D. Krstic based on the method of least squares fitting of a straight line.

## DISCUSSION AND CONCLUSIONS

Inspection of the data plotted on the concordia diagram in Figure 5 reveals a typical discordance relationship, with a single straight line fit to the data points having an upper and lower intercept (with the concordia). The mean square weight of deviates (MSWD) of this line, at



Sample Number	$^{238}\text{U}$ , ppm	$^{235}\text{U}$ , ppm	$^{206}\text{Pb}$ , ppm	$^{207}\text{Pb}$ , ppm	Measured atomic ratios, Pb $^{206}/^{204}$	$^{207}/^{206}$
IZ 1-6 xenotime	1150.7	8.2	173.4	12.7	16949 + 575 —	0.07317 + 0.00001 —
IZ 1-8 euxenite	97554.0	698.6	15236.9	1150.5	14493 + 420 —	0.07514 + 0.00002 —
IZ 3-2 euxenite	86044.7	616.2	10878.3	789.8	11905 + 142 —	0.07225 + 0.00006 —
IZ 3-2 euxenite	79235.4	567.4	10177.9	740.1	7194 + 259 —	0.07237 + 0.00001 —
IZ 3-3 euxenite	78903.7	565.1	11833.0	885.8	15385 + 237 —	0.07453 + 0.00004 —
IZ 3-4 euxenite	95793.0	686.0	12572.7	918.3	43478 + 3781 —	0.07268 + 0.00003 —
WZ-2 euxenite	106249.	760.9	15559.9	1148.3	8248 + 205 —	0.07344 + 0.00001 —

TABLE 3. U/Pb analytical data for minerals from the Gloserheia pegmatite.



Sample Number	DATE*, m.y.		ATOMIC RATIOS	
	206/208	207/235	206/238	207/235
IZ 1-6 xenotime	1035	1030	0.1741	1.7565
IZ 1-8 euxenite	1069	1070	0.1805	1.8695
IZ 3-2 euxenite	874	912	0.1461	1.4551
IZ 3-2 euxenite	892	923	0.1484	1.4808
IZ 3-3 euxenite	1030	1042	0.1733	1.7883
IZ 3-4 euxenite	910	938	0.1516	1.5197
WZ-2 euxenite	1008	1014	0.1692	1.7133

\* constants used in calculating these dates are given in the text.

TABLE 4. U/Pb apparent dates and analytical data for minerals from the Gloserheia pegmatite.









5.3, is higher than the upper limit accepted for an isochronous relationship, so the scatter about the regression line is probably related to a geological disturbance. Still, it may be concluded that the uranium mineralization occurred as a single event  $1055 \pm 30$  m.y. ago. The samples have lost only small amounts of radiogenic lead. Perusal of the isotopic abundance data in Tables 3 and 4 reveals no correlation between uranium content and the degree of discordancy, although this correlation is frequently observed in zircons. The euxenite samples show the 'normal' or zircon lead loss pattern while the xenotime shows the reverse discordancy pattern usually caused by U loss (Cobb and Kulp, 1961; Catanzaro, 1968; Tilton and Nicolaysen, 1957).

On the concordia plot (Figure 5), the uppermost data points show slight scatter about any discordia that may be constructed. The cluster of data points about the upper intercept of the discordia increases the uncertainty of the lower intercept. The significance of the lower intercept, which indicates a date of  $403 \pm 160$  m.y., is unclear in an episodic lead loss interpretation. It corresponds roughly to the time of the Caledonian in the Baltic Shield, although there is no documented evidence for Caledonian events in this area. The Rb-Sr data of this study do suggest a late low-grade metamorphic event of uncertain age which could furnish evidence of Caledonian effects. Extrapolation of the linear portion of a continuous diffusion trajectory would have a slightly lower intercept than the intercept observed in Figure 5. This same ambiguity in interpretation is paralleled in the findings of O'Nions and Baadsgaard (1971) for other pegmatites in the Kongsberg-Bamble sector. Most probably this pattern has been produced by continuous diffusion of lead from mineral lattices coupled with very low-grade



events that caused episodic lead loss. Examination of the thin sections of the rocks containing these minerals suggests that there has been limited hydrothermal activity that would facilitate leaching of lead and uranium. Because of the commonly observed correlation between the degree of lattice damage (metamictization by U decay) and the amount of lead loss, the only minor amounts of radiogenic lead lost by the euxenite samples suggests that any episode of lead loss occurred fairly shortly after crystallization.

In conclusion, the U-Pb data suggests that the uranium minerals formed in a single event at  $1055 \pm 30$  m.y. The age patterns shown by the minerals suggest that lead loss has occurred in response to a series of very low grade events fairly shortly after crystallization (although the possibility exists that this event was as late as the Caledonian) of the pegmatite, coupled with continuous diffusion of lead from the mineral lattices.





## CHAPTER VI OXYGEN ISOTOPE GEOCHEMISTRY

### INTRODUCTION

Oxygen is a major constituent of most rock forming minerals. The oxygen isotope composition of rocks and minerals can provide significant information regarding the conditions of formation of igneous, metamorphic and sedimentary rocks. Additionally, measurement of oxygen isotope ratios is an important technique by which interaction between an oxygen bearing fluid or gas and a rock is discernible.

The purpose of this study is to obtain information regarding the genesis and geological history of the Gloserheia pegmatite. The isotopic composition of the pegmatite may indicate if its parent material was of an igneous or sedimentary nature. Equilibrium fractionations in oxygen isotope distribution between mineral phases can be used as a geothermometer to indicate the temperatures and sequence of crystallization of the zones. Alternatively, if these patterns have been obliterated through subsequent isotopic exchange with circulating meteoric groundwaters or deuteritic fluids, the nature, effect, and degree of exchange with these fluids can be deduced.

### OXYGEN ISOTOPE SYSTEMATICS

Detailed discussions of oxygen isotope geochemistry can be found in reviews published by Epstein (1959), Epstein and Taylor (1967), Garlick (1969), and Faure (1977). Brief summaries of the basic principles and of the behavior of isotopes during fractional crystallization are presented here, in addition to a review of recent literature concerning oxygen isotopes in pegmatites.



### (i) General theory and applications

Variations in the oxygen isotope ratios of natural substances arise from the differences in the thermodynamic and kinetic properties of the various isotopic species in chemical compounds. The differences occur primarily because of the effect of mass. The isotopic composition of oxygen is usually expressed as  $^{18}\text{O}$  and reported with respect to standard mean ocean water (SMOW, Craig, 1961):

$$\delta^{18}\text{O} = \left[ \frac{^{18}\text{O}/^{16}\text{O}_{\text{sample}}}{^{18}\text{O}/^{16}\text{O}_{\text{SMOW}}} - 1 \right] \times 1000$$

As early as 1951 it was noted that granites ( $\delta^{18}\text{O}$  7‰) are more enriched in  $^{18}\text{O}$  than mantle rocks ( $\delta^{18}\text{O}$  5-6‰) (Silverman, 1951). Since then considerable effort has been addressed towards resolving the cause of this variation, which could be produced either through fractional crystallization or through magmatic assimilation and interaction with pre-existing supracrustal rocks. Fractional crystallization accounts for some granites, but can only produce isotopic enrichment of up to 8‰, because at magmatic temperatures isotopic fractionation factors are small (Garlick, 1966). Many plutons, however, have  $\delta^{18}\text{O}$  ratios in excess of 10‰ (Longstaffe et al, 1981). For these plutons, the second hypothesis seems reasonable. Supracrustal rocks, and in particular clastic sediments, are commonly enriched in  $^{18}\text{O}$ , and this is attributed to the presence of clay minerals derived through weathering processes (Savin and Epstein, 1970). A mantle derived magma would have to incorporate a great quantity of  $^{18}\text{O}$ -rich crustal rock to produce the degree of  $^{18}\text{O}$  enrichment observed in some plutons, so assimilation is not regarded as a feasible process (Taylor, 1968). However, two very attractive hypotheses remain: (i) widespread oxygen isotope exchange of



a magma with the surrounding country rock through a fluid phase; and (ii) the generation of a melt through anatexis of clastic sediments. Through detailed study of the chemistry of the granitic and country host rocks it may be possible to discern which of these two processes has operated.

The second major use of the study of oxygen isotopes is to determine whether isotopic equilibrium was achieved and preserved in a given system. Equilibrium in a granitic rock at the time of crystallization is expressed by a  $\delta^{18}\text{O}$  whole rock value that falls within a fixed range of +6 to +10 ‰ (Taylor, 1978). Variation within this range is attributed to the  $^{18}\text{O}$  content of the parent magma, differences in the temperature of crystallization, and the effect of fractional crystallization. Secondly, igneous and metamorphic rocks in isotopic equilibrium show a characteristic pattern of decreasing  $^{18}\text{O}$  content in their component minerals: quartz-potassium feldspar-plagioclase-muscovite-hornblende-biotite-magnetite (Taylor and Epstein, 1962). The difference in  $^{18}\text{O}$  between any two of these minerals (reported as the  $\Delta^{18}\text{O}$  value) is fixed within a narrow range and is controlled essentially by temperature.

This relationship has found an important application in geothermometry. Equilibrium fractionation factors have been calibrated in laboratory experiments in such a way as to permit systematic treatment of isotopic data and to provide geologically reasonable 'temperatures of formation' for a variety of mineral pairs (Taylor, 1968). For  $N$  mineral phases,  $N-1$  independent temperatures may be deduced, and if these are in accord, and if the isotopic composition has not shifted subsequently to the completion of crystallization, it may be concluded





that isotopic equilibrium was attained. However, the petrogenetic significance of these temperatures is unclear. Some degree of exchange subsequent to initial crystallization is probable and depends on the nature and volume of the fluid phase, so that the temperatures obtained probably represent the temperatures of final equilibration (Bottinga and Javoy, 1975).

Equilibrium may not exist if exchange reactions did not attain equilibrium at the time of crystallization, or if the isotopic composition of a mineral or rock subsequently shifted, due to interaction and exchange with circulating deuteritic or meteoric waters. On a gross scale, bulk readjustment may be expressed by variation of  $^{18}\text{O}$  outside of the normal range for plutonic rocks. On a smaller scale, ie. within a given body, disequilibrium may be expressed by variation in the  $^{18}\text{O}$  composition of rock samples from different locations, and on the scale of minerals, by reversal of the characteristic sequence of  $^{18}\text{O}$  enrichment. Subtle readjustments may be indicated by variation in the delta ( $\Delta$ ) value outside of the permitted range (which varies for each mineral pair), or expressed as discordance in crystallization temperatures calculated for mineral triplets.

The most common cause of disequilibrium is late stage, low temperature exchange with deuteritic or meteoric water, either during crystallization or subsequent to its completion (Taylor, 1978). Deuteritic waters are characteristically  $^{18}\text{O}$  enriched, and their composition may be determined either by magmatic composition coupled with the effects of fractional crystallization, etc., or these waters may be in equilibrium with country rock, which may have a significantly different isotopic composition from the intruding body. Meteoric waters



are markedly depleted in  $^{18}\text{O}$  with respect to igneous and metamorphic rocks (Craig, 1961), and the effect of interaction with rocks is pronounced depletion of  $^{18}\text{O}$  (in the rocks) (Magaritz and Taylor, 1976).

## (ii) Fractional crystallization

Fractional crystallization is commonly invoked as the mechanism responsible for zonation on all scales of igneous bodies. Jahns and Burnham (1969) call upon fractional crystallization to produce zoning in complex granitic pegmatites. This same process is also regarded as a mechanism that operates to produce oxygen isotope variation in a crystallizing magma. As such, the process merits at least precursory consideration.

In a magma, early crystallizing phases are  $^{18}\text{O}$  poor, and crystallization of such minerals relatively enriches the remaining melt. The degree of enrichment is a function of the type of minerals crystallizing, the sequence of crystallization, the temperature of formation, and the extent to which crystallizing minerals are prevented from interaction with the melt through armouring or crystal settling. These factors vary in turn with magmatic composition,  $P_{\text{H}_2\text{O}}$ , oxygen fugacity, melt viscosity, etc. The final isotopic composition of the crystalline product is the result of complex interaction of many variables, and as such is difficult to predict.

Fractional crystallization of a volatile-rich magma commonly leads to separation of an aqueous vapor phase, either through degassing of assimilated country rock, or through saturation with volatiles and resurgent boiling. This aqueous phase can cause appreciable isotopic readjustment through exchange reactions with silicate melt and previously crystallized material. This exchange is likely to



continue at temperatures significantly lower than the temperature of initial separation of the vapor phase or the temperature of crystallization of major minerals. The effects of this process would be a pronounced positive enrichment in the  $\delta^{18}\text{O}$  composition in the exchanged rock. (Taylor, 1968).

The Muskox Intrusion of the Northwest Territories of Canada is a well documented classic example of fractional crystallization of a magma of basaltic composition. The oxygen isotope data shows a progressive upward enrichment from 6.2 to 12.3 ‰, corresponding to rock types representing increasing degree of differentiation (Epstein and Taylor, 1967). Although the fractionation factors are too large to be reconciled with simple crystal-melt equilibria, fractional crystallization has undoubtedly played a role in producing the trends observed in the lower portion of the body (Taylor, 1968). Isotopic analysis of the minerals in the anomalously  $^{18}\text{O}$  rich upper portion of the intrusion suggests that the feldspars, which are in disequilibrium, are responsible for the whole-rock enrichment. It must be concluded that some additional process of  $^{18}\text{O}$  enrichment has been in operation. Taylor (1968) suggested that this trend is the product of post-crystallization exchange with an oxygen-enriched fluid phase that may well have been produced by magmatic differentiation. O'Neil and Taylor (1967) have demonstrated that feldspars exchange oxygen much more readily than quartz under experimental conditions, and that exchanged feldspars, which are typically turbid and filled with fluid inclusions, texturally resemble 'natural' feldspars with anomalous isotopic ratios.

In conclusion, it seems likely that fractional crystallization exerts a pronounced effect both through changes due to gradual shifts





in bulk chemistry, and through formation of a highly corrosive and reactive aqueous phase that may persist to hydrothermal temperatures. The effects of these processes have been considered for ingeous bodies on the scale of plutons. The role of these processes during pegmatite crystallization must be considered next.

(iii) Oxygen isotope literature concerning pegmatites

Granite pegmatites show a more complex variation in oxygen isotope composition than normal plutonic granitic rocks. Many pegmatites are found to be highly enriched in  $^{18}\text{O}$  ( $\delta^{18}\text{O}$  8 ‰) relative to average granitic rocks ( $\delta^{18}\text{O}$  7-11 ‰)(Taylor and Epstein, 1963; Taylor, 1968; Longstaffe et al, 1980). Oxygen isotope composition of component minerals also reflects this range.  $\delta^{18}\text{O}$  values of pegmatitic quartz are reported in the literature as ranging from +8.2 to 13.5 ‰.(Taylor and Friedrichsen, 1978; Longstaffe et al, 1980), with variations of up to 1.1 ‰ in quartz and in feldspar within a single body (Taylor and Epstein, 1962; Taylor et al, 1978). This contrasts sharply to the narrow range exhibited by 'normal' pristine granitic rocks.

In individual bodies, quartz and feldspar in the first intermediate zone and core have been observed to show disequilibrium fractionations ranging between +0.4 and +1.5 ‰. This is interpreted as the result of crystallization from two coexisting phases. More often, these fractionations are not observed, and the  $^{18}\text{O}$  values of minerals suggest that isotopic exchange with wall rock has masked the original distribution.

Longstaffe et al (1980, 1981), in a study of the Manitoba pegmatite district, have demonstrated variable degrees of  $^{18}\text{O}$  exchange between four related pegmatitic granites and their host rocks, with the degree of enrichment of the pegmatites related to the composition of the host



rock: specifically, with the greatest enrichment occurring in pegmatites hosted in meta-greywackes and the least enrichment in metabasalts. Taylor et al (1978) make the same observation for a suite of Californian pegmatites. The explanation for this trend is exchange through supercritical fluids produced during crystallization of volatile saturated (granitic) magmas.

This type of exchange, of course, invalidates a geothermometric approach to a detailed, zonal, cooling history. However, in some cases mineral equilibrium may be demonstrated and suggests supersolidus crystallization in the  $750^{\circ}$ - $580^{\circ}$ C range with gradations in temperature indicating crystallization from the walls inward. In addition, Taylor et al (1978) have suggested that the conditions (pressure and temperature) during crystallization would be appropriate for the formation of aplite with a sudden slight release of pressure.

The recent literature supports Jahns and Burnham's (1969) model of magmatic origin for complex pegmatites with fractional crystallization and development of a supercritical aqueous phase, facilitating isotopic exchange with surrounding rock.

### SAMPLES

Quartz, potassium feldspar, biotite and muscovite were selected for oxygen isotope determination. The mineral phases are distributed ubiquitously throughout the pegmatite, and with the exception of quartz, these same minerals have been analysed for rubidium and strontium isotopic composition.

Minerals from three rock samples from different zones in the pegmatite were analysed for isotopic equilibrium. This determination is usually based on the analysis of mineral triplets (in a rock) but a



limitation was imposed on this study in that only three of the hand specimens contained appropriate mineral distributions. In addition, two quartz-muscovite pairs and five single quartz samples from various locations within the pegmatite, and two fine-grained host rock amphibolites from the contact aureole were analysed.

Detailed descriptions of the samples are located in Appendix A. The amphibolites were quite fresh. The pegmatite samples (in thin section) tended to be fractured and (excepting quartz) altered. Feldspar showed limited alteration to sericite and carbonate, and the biotite was weakly chloritized. Both micas showed signs of stress, with warped, and in biotite only, secondary cleavages.

#### ANALYTICAL

The crushing, separation and purification procedures are outlined in Appendix B.

The samples were analysed by the  $\text{BrF}_5$  method of Clayton and Mayeda (1963). The data is reported with respect to SMOW (Craig, 1961) in the usual  $\delta$  notation. The deviation of  $\pm 0.1\%$  was calculated from the pooled residual variance of replicate analyses (of other samples) performed by Dr. K. Muehlenbachs during the course of this work.

#### RESULTS

The experimental data and the temperatures calculated on the basis of mineral pair fractionation data are reported in Table 5. Temperatures are calculated using the oxygen isotope thermometry equations of Bottinga and Javoy (1973). Approximations of the reliabilities of the  $\delta^{18}\text{O}$  values and the temperatures are included in the table. For ease of intercomparison of the samples, the data is





Sample	Quartz (+0.1%)	K-Feldspar (+0.1%)	Biotite (+0.1%)	Muscovite (+0.1%)	$\Delta^{18}\text{O}$ (+0.1%)	Temperature (°C)
C-1	+12.8‰			+ 9.3‰	(Q-M) 3.5	460° +25°
C-4	+10.8‰					
C-5	+11.4‰					
C-6	+11.2‰					
C-7	+11.7‰					
CI-1	+10.6‰	+10.1%	+ 7.1‰		(Q-K) 0.5 (Q-B) 3.5	1000° +? 680° +40°
IZ1-2	+10.5‰					
IZ1-11	+11.9‰	+10.5‰	+ 7.5‰		(Q-K) 1.4 (Q-B) 4.4	570° +60° 580° +25°
IZ2-1	+11.4‰			+ 9.7‰	(Q-M) 1.7	730° +50°
IZ4-1	+11.3‰	+ 9.2‰	+ 5.5‰		(Q-K) 2.1 (Q-B) 5.8	410° +50° 480° +25°
TOTAL RANGE	2.3‰	1.3‰	2.0‰	0.4‰		

TABLE 5.  $^{18}\text{O}/^{16}\text{O}$  ratios for minerals from the Gloserheia pegmatite.  
( $^{18}\text{O}/^{16}\text{O}$  reported with respect to SMOW)



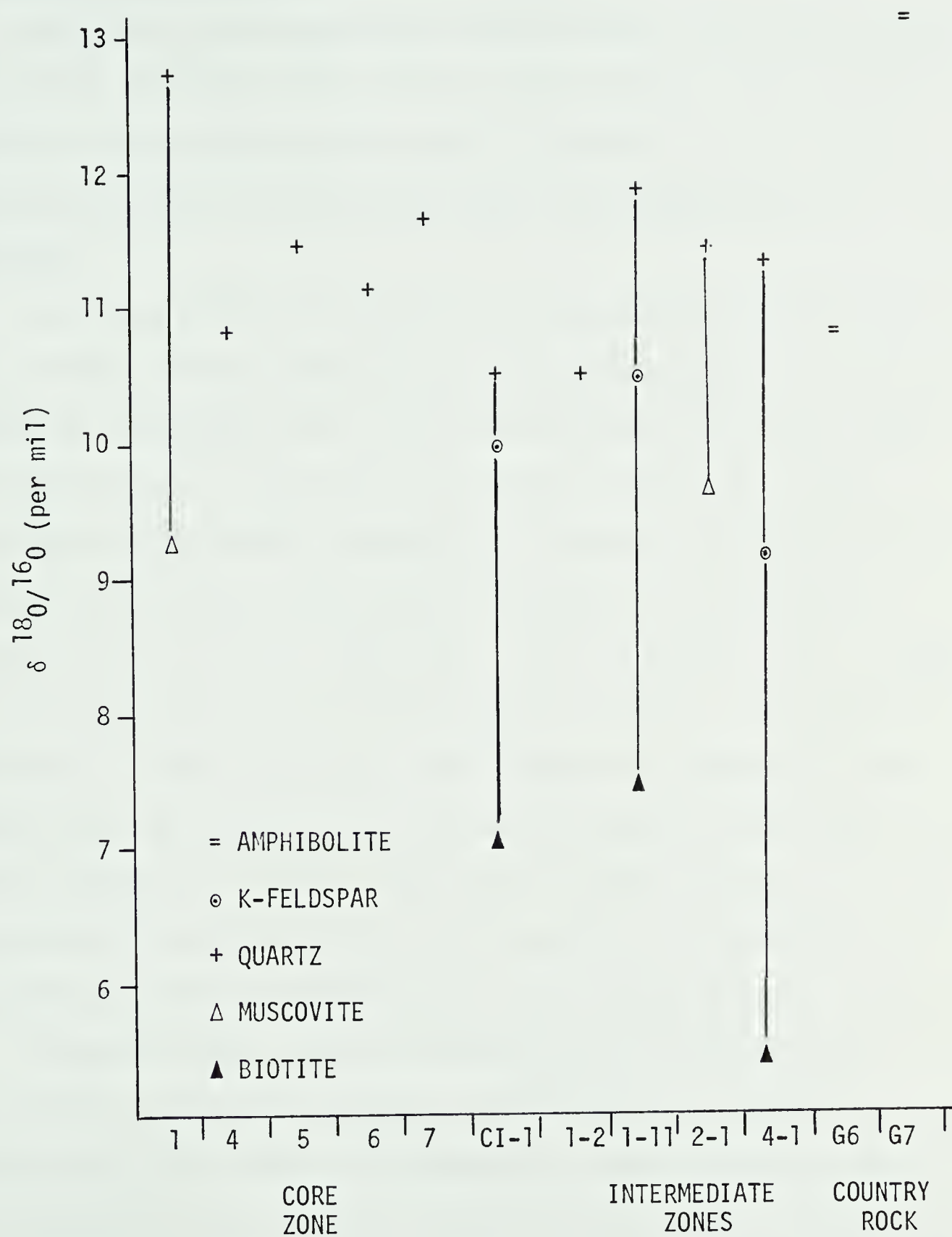


FIGURE 7. Oxygen isotope analyses of minerals from the Gloserheia pegmatite and surrounding amphibolite.



graphically presented as mineral  $\delta^{18}\text{O}$  composition related to zone distribution in Figure 7.

### DISCUSSION AND CONCLUSIONS

Inspection of the experimental data shows that the oxygen isotopes are strongly enriched in  $^{18}\text{O}$  relative to most granitic rocks, and fall within the range established for granitic pegmatites. On this basis, the possibility of interaction with meteoric groundwaters may be dismissed.

The mineral  $\delta^{18}\text{O}$  values are all of the appropriate magnitude, but the variations between samples of the same mineral phase are large and outside of experimental error. For example, quartz  $\delta^{18}\text{O}$  values range from 10.5 to 12.8 ‰, and the net variation is double the maximum predicted variation within a given body. Moreover, a variation of 1.2 ‰ occurs in the core zone alone, which is expected to be uniform with respect to oxygen isotope composition. Quartz is reputed to be a stable mineral which does not (relatively) exchange isotopes. The variations observed in feldspar and biotite are of comparable magnitude but these minerals have been demonstrated to characteristically exhibit such ranges (Taylor et al, 1978). The variation suggests either disequilibrium processes during crystallization or late deuteric alteration has locally readjusted the isotopic composition.

The normal oxygen isotope enrichment pattern of minerals is observed for those phases analysed, with  $\delta^{18}\text{O}$  values increasing progressively in the order biotite-muscovite-potassium feldspar-quartz. It is significant that no quartz-feldspar reversals occur. Large scale low temperature hydrothermal alteration is readily recognizable through such reversals. As previously discussed, feldspars particularly show





this effect as they are readily susceptible to clay alteration, and because they exchange oxygen more rapidly than quartz or mafic minerals (O'Neil and Taylor, 1967). Expected systematic trends in isotopic fractionation between mineral pairs from different zones have either not developed or have been masked by a later process. The three quartz-feldspar pairs analysed in this study all have  $\Delta$  values within the expected range of 0.8 to 2.0 (O'Neil and Taylor, 1967). Only one of the three quartz-biotite pairs analysed (IZ 1-4, with a  $\Delta$  value of 5.8) falls outside of the established  $\Delta$  value range of 3 to 5 (O'Neil et al, 1977). Biotite is a hydrous mineral and is susceptible, like feldspar, to secondary alteration. The altered nature of the biotite (in this study) is apparent during inspection of the thin sections. Equilibrium quartz-muscovite fractionations have been demonstrated to range from 2 to 5 (O'Neil and Taylor, 1969), and two pairs analysed fall well within this range.

The erratic distribution of oxygen isotopes suggest that the conditions for meaningful application of geothermometry have been violated, viz. the isotope composition of a mineral or rock must not in any way have shifted subsequent to the attainment of equilibrium during crystallization from a magma. Therefore, the significance of the temperatures obtained from mineral pair fractionations is questionable. Of the triplets analysed, one (IZ 1-11) closely approached isotopic equilibrium and suggested a temperature of 575<sup>0</sup>C. It may represent the temperature at which oxygen isotope exchange ceased. This temperature does fall neatly within the range suggested by Jahns and Burnham (1969) and agrees with the experimental data of Taylor et al (1978).

In summary, the pegmatite may have formed either through



differentiation from a juvenile igneous source, followed by isotopic exchange with or assimilation of metasedimentary host rocks, or through anatexis of  $^{18}\text{O}$  enriched metasedimentary material. Assimilation of host rock is considered less likely because of the lack of xenoliths in the Gloserheia pegmatite. This is not expected, in any case: Taylor et al (1978) report that (generally) no correlation exists between the bulk chemistry of a pegmatite and its host rock for any known occurrence. Metasedimentary origin of the magma can only be properly evaluated with the assistance of other isotopic or petrographic data. The collected isotopic and petrographic data will be considered in the following chapter.

The disequilibrium redistribution of isotopes was probably largely facilitated by the presence of an aqueous vapor phase created through resurgent boiling. This phase would have been highly corrosive to previously crystallized minerals. Because it would have persisted to lower temperatures than the crystallizing temperatures of the minerals, this fluid or vapor phase would be expected to locally cause  $^{18}\text{O}$  enrichment through isotopic exchange. This mechanism has been invoked by Taylor and Friedrichsen (1978) and Longstaffe et al (1980, 1981) to account for anomalous oxygen isotope distribution in other pegmatites.

This same phase would be expected to facilitate isotopic exchange of the pegmatite minerals with the amphibolitic wall rock ( $\delta^{18}\text{O}$  10.8 and 13.2 ‰, two analyses). Factors that Turi and Taylor (1971) consider to promote this exchange are (1) the volume of the intrusion is small in comparison with the host rock; (2) the late to post tectonic environment would still be quite hot and (3) abundant volatiles would be associated with pegmatitic intrusions. The effect on a juvenile



igneous magma (  $\delta^{18}\text{O}$  7-8 ‰ ) would be quite pronounced with a difference of about 6 ‰ between the intrusion and the wall rock. At the same time to produce such a large isotopic shift a very large volume of wall rock would have to be exchanged, and one would expect to see effects attributable to deuteric alteration in the amphibolite. It is regarded as unlikely that this was the case. However, the effects of wall rock exchange on a metasedimentary magma would be almost negligible. This exchange would have the important effect of resetting any original zonal distribution and account for the disequilibrium observed.

In spite of the significance of these departures from equilibrium, fractionations, the variations are still quite small. Alteration of the pegmatite by meteoric waters or weathering processes is precluded by the strong positive enrichment of  $\delta^{18}\text{O}$  and its distribution in various mineral phases. The  $\delta^{18}\text{O}$  values show at least an approach to equilibrium, and the isotopic composition of the minerals may be assumed to reflect the composition of the melt itself.





## CHAPTER VII SUMMARY AND CONCLUSIONS

The various mineral phases of the Gloserheia pegmatite ( a complex granitic pegmatite in South Norway) were analysed for their radioisotope composition using the Rb-Sr and U-Pb geochronological methods, and for their oxygen isotope geochemistry. The study was undertaken to establish the age of the pegmatite and to relate it to the geological history of the Bamble sector of the Baltic Shield; and to determine the factors governing the emplacement of the pegmatite. During the course of the study it became apparent that open-system behavior significantly modified at least the original isotope distribution, so the events that might have contributed to the final isotopic pattern were considered.

The complete suite of Rb-Sr isotope data for the Rb-bearing mineral phases yielded a "scatterchron" when plotted on a Nicolaysen diagram; however an isochron could be fitted to the relatively unaltered (dominantly potassium feldspar) mineral samples. The date calculated from the isochron indicated that these samples began to behave as a closed system  $1009 \pm 6$  m.y. ago. The oligoclase, muscovite, and biotite samples, comparatively sensitive to updating during subsequent metamorphic events, scatter mostly below the reference isochron with the exception of the very low Rb and Sr-bearing oligoclase samples, which scatter above the isochron near its intercept. It is concluded that some low grade event resulting in alteration and incomplete isotopic rehomogenization occurred after 1009 m.y., with probable redistribution of Rb,  $Sr_N$ , and  $^{87}Sr_r$  between the various more 'sensitive' mineral phases.

While the Rb-Sr mineral isochron yields one date, the U-Pb concordia plot may yield two: the time of formation of a system, and the time of



subsequent metamorphism. The U-Pb data for euxenite and xenotime suggest a crystallization date of  $1055 \pm 30$  m.y. The samples are discordant, with euxenite showing the common lead-loss pattern, and xenotime showing 'reverse' discordancy typical of uranium loss. The significance of the lower intercept of the discordia, which indicates an event at 403 m.y., is unclear. This was about the time of the Caledonian orogeny in the Baltic Shield, but no evidence for this event is documented in the area. The intercept is slightly higher than the extrapolated linear portion of a continuous diffusion trajectory. The discordia pattern can be produced by continuous diffusion of lead from the mineral lattices coupled with a very low grade event causing minor episodic lead loss.

The U-Pb date is significantly (outside of analytical error) older than the Rb-Sr date. However, the Rb-Sr date is calculated from a mineral isochron, and as such could only be expected to yield the last date at which the mineral lattice closed to the migration of radio-isotopes. It seems unreasonable that the uranium mineralization would predate crystallization of the silicate minerals of the pegmatite body. It is more likely that the pegmatite was emplaced at the date indicated by the U-Pb method, and that subsequent metamorphic pulses continued to disturb the system, with the last major pulse occurring at 1009 m.y. Very low grade events continued to disturb the system, causing Rb and Sr isotopic redistribution in the micas and the plagioclase and causing minor Pb and/or U loss in the uranium-bearing minerals.

This interpretation accords well with the literature concerning the Sveco-Norwegian event in the Bamble-Kongsberg sector (of the Baltic Shield). O'Nions (1969) and Field and Råheim (1979) suggested that this



orogeny occurred between 1100 and 1000 m.y., with major and minor pulses of metamorphic activity through this time period. It is speculated that the subsequent minor disturbance of the radioisotopes occurred during intrusion of the post-kinematic granitic plutons in the region.

The source of the magma may be indicated by consideration of the oxygen isotope composition together with the  $^{87}\text{Sr}/^{86}\text{Sr}$  ratio at the time of crystallization of the mineral phases. If the U-Pb date is accepted as the age of crystallization of the pegmatite, the  $^{87}\text{Sr}/^{86}\text{Sr}$  ratio indicated by the intercept of the isochron must be corrected for the amount of radiogenic Sr formed in the interval between 1055 and 1009 m.y. This can only be roughly approximated by assuming the  $^{87}\text{Rb}/^{86}\text{Sr}$  ratio of the pegmatite to be within the range of 6 to 12. This range in composition would produce an initial ratio (at 1055 m.y.) of between 0.705 and 0.709. The lower ratio is typical of mantle-derived igneous material. Alternatively Field and Raheim (1979) present Sr isotopic ratios in this range for older (about 1600 m.y.) very low Rb ( $\text{Rb}/\text{Sr} \sim 0.05$ ) amphibolite and granulite facies rocks in this sector of the Baltic Shield.

Oxygen isotope data and consideration of the petrography of the pegmatite body make it possible to realistically evaluate these two possibilities. The factors that govern the enrichment -or depletion- of strontium isotopes in geological material are entirely unrelated to the processes that govern oxygen isotope fractionation: sialic crustal material is enriched in radiogenic Sr because of the decay of radioactive Rb, while continental sedimentary rocks are  $^{18}\text{O}$  enriched through low temperature alteration processes. Evaluation of the distribution of





these isotopes may make it possible to discern the degree of contamination and interaction with (sialic) crustal material. The oxygen isotope composition of silicate mineral phases of the Gloserheia pegmatite are significantly enriched in  $^{18}\text{O}$  in comparison to 'juvenile' igneous granitic rocks. Moreover, the oxygen isotope composition of amphibolites are of the same approximate range as the Gloserheia pegmatite. Secondly, the pegmatite contains biotite and muscovite as major mineral components. The presence of two micas is usually considered to indicate metasedimentary origin. A primary mantle source for the pegmatite cannot be absolutely dismissed, but for the above reasons, the preferred source for the magma is anatexis of pre-existing Rb depleted,  $^{18}\text{O}$  enriched amphibolitic parent.

One of the major aims of this study was to correlate isotopic distributions to the internal zones developed in the Gloserheia pegmatite. However, during the course of analysis it became apparent that if such correlations existed they had not been preserved. The U-bearing minerals had suffered U and/or Pb loss, the micas and feldspars were visibly altered and had suffered variable Rb and/or Sr isotope redistribution, and the oxygen isotopes of even very closely spaced samples showed marked disequilibrium fractionations.

Oxygen isotope disequilibrium fractionations in pegmatite bodies are commonly attributed to interaction of crystalline mineral phases with a highly corrosive supercritical aqueous fluid or vapor, produced during fractional crystallization as a result of volatile saturation of the magma. This may facilitate local exchange between the vapor or fluid phase and previously crystallized minerals, and secondly, it may facilitate exchange with the wall rock, for while the more viscous



silicate magma would be contained by the enclosing wall rock, the much less viscous, highly volatile aqueous phase would not, and would act as a medium for the exchange between the pegmatite minerals and the wall rock. These processes may well have contributed to the oxygen isotope disequilibrium fractionations observed in the Gloserheia pegmatite. However, the Rb-Sr and U-Pb systems have also been disturbed at a sufficiently later time to cause significant loss of radiogenic isotopes. It seems reasonable that an event disturbing these systems would also affect the oxygen isotope distribution. Interaction with meteoric water has been dismissed on the basis of the  $^{18}\text{O}$  enriched nature of the mineral phases of the Gloserheia pegmatite. Low temperature hydrothermal alteration would be expected to cause (unobserved) reversals in the  $^{18}\text{O}$  fractionation between quartz and feldspar. Presumably, then, the hydrothermal event disturbing the isotope systematics was relatively high temperature and may well have affected all the mineral phases, not just the feldspars.

The nature of such a fluid is at best speculative. Burnham (1967) has demonstrated that aqueous phases coexisting with magmas or igneous rocks at high temperatures tend to strongly partition alkali chlorides. Such solutions would be expected to be enriched in K and Na, at least when in contact with granitic rocks, and to be highly corrosive, preferentially causing selective replacement of feldspars (Robertson, 1959) and modifying the alkali content of the body as a whole (Taylor and Forester, 1971; O'Neil and Taylor, 1967). Such exchange requires the breaking of bonds, and it is likely that cation exchange (including Rb, Sr, and Pb) would be accompanied by oxygen isotope exchange.

O'Neil and Taylor (1967) considered the mechanics of such hydro-



thermal cation exchange, proposing a solution-redeposition model, with a reaction front sweeping through crystal lattices along lattice defects in response to disequilibrium conditions. They suggest that cation (Na, K) exchange provides the "driving force" for oxygen isotope exchange between feldspars and fluids during deuteritic, hydrothermal, and metamorphic processes. A highly similar mechanism has been more recently proposed by Giletti et al (1978).

Several geological examples of problematic distribution of Rb, Sr, Pb, and oxygen isotopes have been interpreted to be the result of such processes. The two best documented cases are the intrusive complexes at Skye, western Scotland (Taylor and Forester, 1971) and the St. Francois Mountains of S. E. Missouri (Wenner and Taylor, 1972, 1976; Bickford and Mose, 1975; Taylor, 1974, 1978). Both complexes have apparently suffered large scale oxygen isotope redistribution. The Tertiary complex at Skye has been  $^{18}\text{O}$  depleted, and the feldspar common lead and Rb-Sr isotope distributions have been disturbed (Taylor and Forester, 1971). The Precambrian St. Francois volcanics and intrusive granites have suffered  $^{18}\text{O}$  enrichment, with feldspar alteration apparently responsible for this trend (Bickford and Mose, 1975; Wenner and Taylor, 1976). Rb-Sr whole-rock dates show a wide range of several hundred million years, and are on the average 11% younger than the U-Pb concordia dates for zircons (Bickford and Mose, 1975). The zircon dates were interpreted as representing the correct time of crystallization of the complex. Recently formed zircons have suffered little radiation damage from U decay, and are considered to be relatively unaffected by hydrothermal events as a result (Taylor, 1974). The variably younger Rb-Sr ages were interpreted to be the result of large





scale open system Sr loss on the basis of a strong positive correlation between Sr content and calculated individual ages. Wenner and Taylor (1972, 1976) proposed that a regional hydrothermal event several hundred million years after the emplacement of the intrusion resulted in feldspar metasomatism and attendant  $^{87}\text{Sr}_r$  loss and  $^{18}\text{O}$  enrichment. The source of the fluids could have been either magmatic or meteoric. The meteoric model would have required significantly different meteoric water isotopic composition than is observed at the present time, but there is no substantiating evidence for this. Consequently the authors prefer a magmatic source for the metasomatizing fluids.

The Gloserheia pegmatite has not been affected by any such pervasive event, but some parallels to the studies of Taylor and Forester (1971), Bickford and Mose (1975) and Wenner and Taylor (1972, 1976) may be drawn. The dates obtained for Rb and U bearing minerals differ slightly but significantly. Rb and Sr isotopes have been redistributed, and the minerals analysed for oxygen isotope composition show isotopic distributions that do not fit normal equilibrium patterns. In thin section, feldspars appear to have been variably metasomatized, the mica cleavages and plagioclase twin lamellae are bent and deformed, and all of the minerals are slightly fractured and hematite stained. The gentle deformation of the minerals may perhaps be attributed to the effects of competing crystallization. The oxygen isotope disequilibrium and the alteration and apparent metasomatism of the feldspars may be related to late hydrothermal activity as a normal stage of pegmatite crystallization in the fractional crystallization model of Jahns and Burnham (1969). U-bearing minerals commonly show lead loss as a result of lattice damage during uranium decay. The only data that cannot be interpreted as resulting from Jahns and Burnham's (1969) model is the Rb-Sr isotope



data. It is difficult to envisage circumstances that would allow Rb-Sr redistribution and correlative feldspar alteration without affecting the oxygen isotope distribution. Perhaps Taylor's (1974) argument for zircon retentivity of lead for a period of time after crystallization may be extended to euxenite, so that the U-Pb concordia date is correct. Reaction with a high temperature hydrothermal fluid causing limited local isotope and cation exchange preferentially along pre-existing fractures would also account for the observed isotope distribution. The effects of such exchange must have been limited and local, for the Rb-Sr, U-Pb and  $^{18}\text{O}/^{16}\text{O}$  isotope content of the body was not homogenized, and no inter- or intracorrelation between the various isotopes is recognizable. The only positive correlation is the degree of alteration of the silicate minerals to the apparent disturbance of isotopic equilibrium.

The disequilibrium isotope distribution that is interpreted to have occurred in response to minor pulses of metamorphic activity makes it difficult to provide clear cut evidence in support of any one model of pegmatite genesis. However, the Gloserheia pegmatite's mineral assemblage and textural relationships support Jahns and Burnham's (1969) model of fractional crystallization from a volatile-rich magma, as does the oxygen and lead isotopic data.

This study demonstrates the importance of the utilization of different methods of investigation in the study of geological material. The use of three different isotope systems removes much of the ambiguity encountered in interpreting the results of one system alone, and provides insight into the complexity of geologic processes and their effect on natural systems.



## REFERENCES

- ÅMLI, R., 1975. Mineralogy and rare earth geochemistry of apatite and xenotime from the Gloserheia granite pegmatite, Froland, Southern Norway. *Am. Mineralogist* 60, 607-620.
- ÅMLI, R., 1977. Internal structure and mineralogy of the Gloserheia granite pegmatite, Froland, South Norway. *Norsk. Geol. Tidss.* 57, 243-262.
- ANDERSON, O., 1926. Feldspat I. *Norg. Geol. Unders.* 128a, 142 p.
- ANDERSON, O., 1931. Feldspat II. *Norg. Geol. Unders.* 128b, 1-109.
- BAADSGAARD, H., 1965. Geochronology. *Medds. fra Dansk., Geol. Foren.* 16, 1-48.
- BAADSGAARD, H., AND VAN BREEMEN, O., 1970. Thermally induced migration of Rb and Sr in an adamellite. *Eclog. Geol. Helv.* 63, 31-44.
- BICKFORD, M. E., AND MOSE, D.G., 1975. Geochronology of Precambrian rocks in the St. Francois Mountains, Southeastern Missouri. *Geol. Soc. Am. Spec. Paper* 165, 48 p.
- BOTTINGA, Y., AND JAVOY, M., 1973. Comments on oxygen isotope geothermometry. *Earth Planet. Sci. Lett.* 20, 250-265.
- BOTTINGA, Y., AND JAVOY, M., 1975. Oxygen isotope partitioning among the minerals in igneous and metamorphic rocks. *Rev. Geoph. Space Phys.* 12, 403-418.
- BROCH, A.O., 1964. Age determination of Norwegian minerals up to March, 1964. *Norg. Geol. Unders.* 228, 84-113.
- BROOKS, C., 1968. Relationships between feldspar alteration and the precise post-crystallization movement of rubidium and strontium isotopes in a granite. *J. Geophys. Res.* 73, 4751-4752.
- BROOKS, C., HART, S.R., AND WENDT, I., 1972. Realistic use of two-error regression treatments as applied to rubidium-strontium data. *Rev. Geoph. Space Phys.* 10, 551-577.
- BRÖTZEN, O., 1959. Outline of mineralization in zoned granitic pegmatites. *Geol. Forën. Stockholm, Förh.* 81, 1-98.
- BUGGE, J. A. W., 1943. Geological and petrographical investigations in the Kongsberg-Bamble formation. *Norg. Geol. Unders.* 160, 150 p.
- BURNHAM, C. W., 1967. Hydrothermal fluids at the magmatic stage. In: *Geochemistry of Hydrothermal Mineral Deposits*, Barnes, H. L. (ed.) Holt, Rinehart, and Winston Inc., N. Y., 34-76.







- CAMERON, E. N., JAHNS, R. H., McNAIR, A.H., AND PAGE, L. R., 1949. Internal structure of granite pegmatites. *Econ. Geol. Monogr.* 2, 115 p.
- CATANZARO, E. J., 1968. The interpretation of zircon ages. In: *Radiometric Dating for Geologists*. Hamilton, E. I., and Farquhar, R. M. (eds.). Interscience, N. Y., 225-258.
- CLAYTON, R. N. L., AND MAYEDA, T. K., 1963. The use of bromine pentafluoride in the extraction of oxygen from oxides and silicates for isotopic analysis. *Geochim. Cosmochim. Acta* 27, 43-52.
- COBB, J. C., AND KULP, J. L., 1961. Isotopic geochemistry of uranium and lead in the Swedish Kolm and its associated shale. *Geochim. Cosmochim. Acta* 24, 226-249.
- CRAIG, H., 1961. Standards for reporting concentrations of deuterium and oxygen-18 in natural waters. *Science* 133, 1833-1834.
- EPSTEIN, S., 1959. The variation of the O-18/O-16 ratio in nature and some geological applications. In: *Researches in Geochemistry*. Abelson, P. H. (ed.), John Wiley, N. Y., 29-62.
- FAURE, G., 1977. *Principles of Isotope Geology*. Wiley and Sons, Toronto, 464 p.
- FAURE, G., AND POWELL, J. L., 1972. *Strontium Isotope Geology*. Springer-Verlag, N. Y., 188 p.
- FIELD, D., AND RÄHEIM, A., 1979. Rb-Sr total rock isotope studies in Precambrian charnockitic gneisses from South Norway: evidence for resetting during low-grade metamorphic deformational event. *Earth Planet. Sci. Lett.* 45, 32-44.
- FLETCHER, R. C., AND HOFMANN, A. W. 1974. Simple models of diffusion and combined diffusion-infiltration metasomatism. In: *Geochemical Transport and Kinetics*. Hofmann, A. W., Giletti, B. J., Yoder, H. S., Jr., and Yund, R. A. (eds.), Carnegie Institution of Washington Publication No. 634, 243-260.
- FOLAND, K. A., 1972. Cation and Ar<sup>40</sup> diffusion in orthoclase. PhD. thesis, Brown Univ., Providence, R. I., 143 p.
- FOLAND, K. A., 1974. Alkali diffusion in orthoclase. In: *Geochemical Transport and Kinetics*. Hofmann, A. W., Giletti, B. J., Yoder, H. S., Jr., and Yund, R. A. (eds.), Carnegie Institution of Washington Publication No. 634, 77-98.
- GARLICK, G. D., 1966. Oxygen isotope fractionation in igneous rocks. *Earth Planet. Sci. Lett.* 1, 361-368.



- GARLICK, G. D., 1969. The stable isotopes of oxygen. In: Handbook of Geochemistry II-1. Wedepohl, K. H. (ed.), Springer-Verlag, N. Y..
- GERLING, E. K., AND OVCHINNIKOVA, G. V., 1962. Causes of low ages determined by the Rb-Sr method. *Geokhimiya* 9, 755-762.
- GILETTI, B. J., 1974. Diffusion related to geochronology. In: Geochemical Transport and Kinetics. Hofmann, A. W., Giletti, B. J., Yoder, H. S., Jr., and Yund, R. A. (eds.), Carnegie Institution of Washington Publication No. 634, 61-76.
- GILETTI, B. J., AND KULP, J. L., 1955. Radon leakage from radioactive minerals. *Am. Mineralogist* 40, 481-496.
- GILETTI, B. J., SEMET, M. P., AND YUND, R. A., 1978. Studies in diffusion-III. Oxygen in feldspars: an ion microprobe determination. *Geochim. Cosmochim. Acta* 42, 45-57.
- GOLDICH, S. S., AND MUDREY, M. G., JR., 1972. Dilatancy model for discordant U-Pb zircon ages. In: Contributions to Recent Geochemistry and Analytical Chemistry. A. P. Vindograv Volume. Tugarinov, A. I., (ed.), Moscow Nauka Publ. Office, 415-418.
- GOLDSCHMIDT, V. M., 1924. "Über die umwandlung krystallisier termierale in de metamikten zustand (isotropisierung). *Skrifter Norske Videnskaps Akad. Kristiania I. Mat.-Naturv. KI No. 5*, Geochemische Verteilung esetze der Elemente III, (Anhang), 51-58.
- GRANDSTAFF, D. E., 1976. A kinetic study of the dissolution of uraninite. *Econ. Geol.* 71, 1493-1506.
- GRESENS, R. L., 1967. Tectonic-hydrothermal pegmatites. *Contrib. Mineral. Petrol.* 15, 345-355.
- HAMILTON, E. I., 1965. Applied Geochronology. Academic Press, London, 267 p.
- HAMILTON, E. I., AND FARQUHAR, R. M., 1968. Radiometric Dating for Geologists. Interscience, London, 506 p.
- HANSON, G. N., 1971. Radiogenic argon loss from biotite in whole rock heating experiments. *Geochim. Cosmochim. Acta* 35, 101-107.
- HART, S. R., 1964. The petrology and isotopic mineral age relations of a contact zone in the Front Range, Colorado. *J. Geol.* 72, 493-525.
- HEIER, K. S., AND TAYLOR, S. R., 1959. Distribution of Li, Na, K, Rb, Cs, Pb, Tl in Southern Norwegian pre-Cambrian alkali feldspars. *Geochim. Cosmochim. Acta* 15, 284-304.
- HOFMANN, A. W., 1969. Hydrothermal experiments on equilibrium partitioning and diffusion kinetics of Rb, Sr, and Na in biotite-alkali-chloride solution systems. PhD. thesis, Brown Univ., Providence, R. I., 105 p.



- HOFMANN, A. W., 1972. Chromatographic theory of infiltration metasomatism and its application to feldspars. *Am. J. Sci.* 282, 69-90.
- HOFMANN, A. W., GILETTI, B. J., YODER, H. S., JR., AND YUND, R. A. (eds.), 1974. *Geochemical Transport and Kinetics*. Carnegie Institution of Washington Publication No. 634, 353 p.
- HOFMANN, A. W., AND GILETTI, B. J., 1970. Diffusion of geochronologically important minerals under hydrothermal conditions. *Eclog. Geol. Helv.* 63, 141-150.
- HOLMES, A., 1955. Dating the Precambrian of peninsular India and Ceylon. *Proc. Geol. Assoc. Canada* 7, 81-106.
- JAFFEY, A. H., FLYNN, K. F., GLENDENIN, L. E., BENTLY, W. C., AND ESSLING, A. M., 1971. Precision measurements of half lives and specific activities of  $^{235}\text{U}$  and  $^{238}\text{U}$ . *Phys. Rev. C* 4, 1889-1906.
- JAHNS, R. H., 1953. The genesis of pegmatites. *Am. Mineralogist* 38, 563-598.
- JAHNS, R. H., 1955. The study of pegmatites. *Econ. Geol.* 50, 1025-1130.
- JAHNS, R. H., AND BURNHAM, C. W., 1969. Experimental studies of pegmatite genesis: a model for the derivation and crystallization of granitic pegmatites. *Econ. Geol.* 64, 843-864.
- KESMARKY, S., 1977. Rates of migration of alkali and strontium ions in a heated quartz monzonite. Unpubl. MSc. thesis, Univ. of Alberta, 107 p.
- KORZHINSKII, V. S., 1965. The theory of systems with perfectly mobile components and processes of mineral formation. *Am. J. Sci.* 263, 193-205.
- KORZHINSKII, V. S., 1970. *The Theory of Metasomatic Zoning*. Clarendon Press, Oxford, 162 p.
- KRATZ, K. O., GERLING, E. K., AND LOBACH-ZHUCHENKO, S. B., 1968. The isotope geology of the Precambrian of the Baltic Shield. *Can. J. Earth Sci.*, 5, 657-660.
- KROGH, T. E., 1973. A low-contamination method for hydrothermal decomposition of zircon and extraction of U and Pb for isotopic age determinations. *Geochim. Cosmochim. Acta* 37, 485-494.
- KULP, J. L., 1955. Isotopic dating and the geologic time scale. *Geol. Soc. Am. Spec. Pap.* 62, 609-630.
- KULP, J. L., AND BASSETT, W. H., 1961. The base-exchange effects on potassium-argon and rubidium-strontium isotopic ages, *Ann. N. Y.*







- Acad. Sci. 91, 225-226.
- KULP, J. L., AND ECKLEMAN, W. R., 1957. Discordant U-Pb ages and mineral type. *Am. Mineralogist*, 154-156.
- KULP, J. L., AND ENGELS, J., 1963. Discordance in K-Ar and Rb-Sr isotopic ages. In: *Radioactive Dating*. International Atomic Agency of Vienna, 219 p.
- LONGSTAFFE, F. J., CERNY, P., AND MUEHLENBACHS, K., 1980. Oxygen isotope variations of pegmatitic granites in the Winnipeg River district, southeastern Manitoba (abs.). *International Assoc. of Geochemistry and Cosmochemistry and the Alberta Research Council, Proc. of the 3rd Int. Symp. on Water-Rock Interaction*.
- LONGSTAFFE, F. J., CERNY, P., AND MUEHLENBACHS, K., 1981. Oxygen isotope geochemistry of the granitoid rocks in the Winnipeg River pegmatite district, southeastern Manitoba. In press.
- MAGARITZ, M., AND TAYLOR, H. P., JR., 1976.  $^{18}\text{O}/^{16}\text{O}$  and D/H studies along a 500 km. traverse across the Coast Range Batholith and its country rocks, central British Columbia. *Can. J. Earth Sci.* 13, 1514-1536.
- McINTYRE, G. A., BROOKS, C., COMPSTON, W., AND TUREK, A., 1966. The statistical assessment of Rb-Sr isochrons. *J. Geophys. Res.* 71, 5459-5468.
- MITCHELL, R. S., 1973. Metamict minerals: a review. Parts I and II. *The Min. Rec.* 4, 177-182, 214-223.
- NEUMANN, H., 1960. Apparent ages of Norwegian minerals and rocks. *Norsk. Geol. Tidss.* 40, 173-189.
- NICOLAYSEN, L. O., 1957. Solid diffusion in radioactive minerals and the measurement of absolute age. *Geochim. Cosmochim. Acta* 11, 41-59.
- NICOLAYSEN, L. O., 1961. Graphic interpretation of discordant age measurements on metamorphic rocks. *Ann. N. Y. Acad. Sci.* 91, 198-206.
- OFTEDAL, L., 1954. Some observations on the regional distribution of lead in South Norwegian granitic rocks. *Norsk. Geol. Tidss.* 33, 153-161.
- O'NEIL, J. R., AND TAYLOR, H. P., JR., 1967. The oxygen isotope and cation chemistry of feldspars. *Am. Mineralogist* 52, 1414-1437.
- O'NEIL, J. R., AND TAYLOR, H. P., JR., 1969. Oxygen isotope equilibrium between muscovite and water. *J. Geophys. Res.* 74, 6012-6022.
- O'NEIL, J. R., SHAW, S. E., AND FLOOD, R. H., 1977. Oxygen and hydrogen



- isotope compositions as indicators of granite genesis in the New England Batholith, Australia. *Contrib. Mineral. Petrol.* 62, 313-328.
- O'NIONS, R. K., 1969. Geochronology of Bamble, South Norway. Unpubl. PhD. thesis, Univ. of Alberta, 172 p.
- O'NIONS, R. K., AND BAADSGAARD, H. B., 1971. A radiometric study of polymetamorphism in the Bamble region, Norway. *Contrib. Mineral. Petrol.* 34, 1-21.
- O'NIONS, R. K., MORTON, R. D., AND BAADSGAARD, H., 1969. Potassium argon ages from the Bamble sector of the Fennoscandian Shield, S. Norway. *Norsk. Geol. Tidss.* 49, 171-190.
- PETROVIC, R., 1974. Diffusion of alkali ions in alkali feldspar. In: *The Feldspars*. Mackenzie, W. S., and Zussman, J. (eds.), Manchester University Press, 174-182.
- POLKANOV, A. A., AND GERLING, E. K., 1961. The Precambrian geology of the Baltic Shield. *Ann. N. Y. Acad. Sci.* 91, 492-499.
- REITAN, P. H., 1965. Pegmatite veins and the surrounding rocks. V. Secondary recrystallization of aplite to form pegmatite. *Norsk. Geol. Tidss.* 45, 31-40.
- ROBERTSON, F., 1959. Perthite formed by reorganization of albite from plagioclase during potash feldspar metasomatism. *Am. Mineralogist* 44, 603-619.
- SAVIN, S., AND EPSTEIN, S., 1970. The oxygen and hydrogen isotope geochemistry of clay minerals. *Geochim. Acta* 34, 25-42.
- SILVERMAN, S. R., 1951. The isotope geology of oxygen. *Geochim. Cosmochim. Acta* 2, 26-42.
- STEIGER, R. H., AND JAGER, E., 1977. Convention on the use of decay constants in geo- and cosmochemistry. *Earth Planet. Sci. Lett.* 36, 359-362.
- TAYLOR, B. E., FOORD, E. E., AND FRIEDRICHSEN, H., 1978. Stable isotope and fluid inclusion studies of gem-bearing granitic pegmatite-aplite dikes, San Diego Co., California. *Contrib. Mineral. Petrol.* 68, 187-205.
- TAYLOR, B. E., AND FRIEDRICHSEN, H., 1978. Stable isotope studies of granitic pegmatites. In: *Short papers of the fourth international conference in geochronology, cosmochemistry and isotope geology*. Zartman, R.E. (ed.), U. S. G. S. Report 78-701, 422-423.
- TAYLOR, H. P., JR., 1968. The oxygen isotope geochemistry of igneous rocks. *Contrib. Mineral. and Petrol.* 19, 1-71.



- TAYLOR, H. P., JR., 1974. Oxygen and hydrogen isotope evidence for large-scale circulation and interaction between ground waters and igneous intrusions, with particular reference to the San Juan volcanic field, Colorado. In: *Geochemical Transport and Kinetics*. Hofmann, A. W., Gilletti, B. J., Yoder, H. S., and Yund, R. A. (eds.), Carnegie Institution of Washington Publication No. 634, 299-335.
- TAYLOR, H. P., JR., 1978. Oxygen and hydrogen studies of plutonic granitic rocks. *Earth Planet. Sci. Lett.* 38, 177-210.
- TAYLOR, H. P., JR., AND EPSTEIN, S., 1962.  $O^{18}/O^{16}$  ratios in feldspars and quartz in zoned granitic pegmatites (abs.). *Geol. Soc. Am. Spec. Paper No. 68*, 283.
- TAYLOR, H. P., JR., AND EPSTEIN, S., 1963.  $O^{18}/O^{16}$  ratios in rocks and coexisting minerals of the Skaergaard intrusion. *J. Petrol.* 4, 51-74.
- TAYLOR, H. P., JR., AND FORESTER, R. W., 1971. Low  $^{18}O$  igneous rocks from western Scotland. *J. Petrol.* 12, 465-497.
- TILTON, G. R., 1960. Volume diffusion as a mechanism for discordant ages in zircons. *J. Geophys. Res.* 65, 2953-2945.
- TILTON, G. R., AND NICOLAYSEN, L. O., 1957. The use of monazites for age determination. *Geochim. Cosmochim. Acta* 2, 28-40.
- TURI, B., AND TAYLOR, H. P., JR., 1971. An oxygen and hydrogen isotope study of a granodiorite pluton from the Southern California Batholith. *Geochim. Cosmochim. Acta* 35, 383-406.
- WASSERBURG, G. J., 1963. Diffusion processes in lead-uranium systems. *J. Geophys. Res.* 68, 4823-4846.
- WENNER, D. B., AND TAYLOR, H. P., JR., 1972.  $O^{18}/O^{16}$  and D/H studies of a Precambrian granite-rhyolite terrane in S. E. Missouri (abs.) *EOS Am. Geophys. Union Trans.* 53, 383.
- WENNER, D. B., AND TAYLOR, H. P., JR., 1976. Oxygen and hydrogen isotope studies of a Precambrian granite-rhyolite terrane, St. Francois Mountains, Southeastern Missouri. *Geol. Soc. Am. Bull.* 87, 1587-1598.
- WETHERILL, G. W., 1956. Discordant uranium-lead ages. *Trans. Am. Geophys. Union* 37, 320-326.
- WETHERILL, G. W., 1963. Discordant uranium-lead ages. Part 2. Discordant ages resulting from the diffusion of lead and uranium. *J. Geophys. Res.* 68, 2957-2965.
- YORK, D., 1966. Least-squares fitting of a straight line. *Can. J. Phys.* 44, 1079-1086.







## APPENDIX A: DESCRIPTION AND LOCATION OF SAMPLES

The pegmatite samples and two host-rock samples made available for study are described below. They are grouped sequentially according to their location within the pegmatite. Sample locations are described in relation to Åmli's (1977) traverses of the central portion of the pegmatite body. Sample locations (where known) are shown in Figure 7.

The specimens are approximately fist-sized. In many cases the minerals are extremely coarse-grained (ranging in size from 1 or 2 up to 10 cm. in length) so that the rock samples are essentially mono- or bi-mineralic. The grain size is generally observed to decrease from the pegmatite core to the outer zones. The dominant mineral found in the core is quartz, with some perthite and muscovite. The intermediate zones consist mainly of biotite or muscovite, feldspar and quartz, with a variety of accessory minerals including carbonate, apatite, sphene, thorite, sphene, euxenite, and uranium secondary minerals. There is abundant evidence of metasomatism, with the development of chessboard replacement-type perthite, muscovite and carbonate replacement of feldspar, ubiquitous iron staining from the breakdown of biotite and other iron oxides, and the presence of uranium secondary minerals. The euxenite in all thin sections is isotropic, indicative of metamict character. The border and wall zones consist mainly of graphic intergrowths of quartz and feldspar. Generally the minerals appear to be quite fresh but thin section analysis reveals that the hand specimen appearance is often misleading.

A representative number of thin sections (21) were cut and examined with a petrographic microscope. Descriptions are included with the appropriate hand specimen descriptions. Mineral abundances were determined by point counting a minimum of 500 points, and are considered to be accurate to  $\pm 5\%$ .

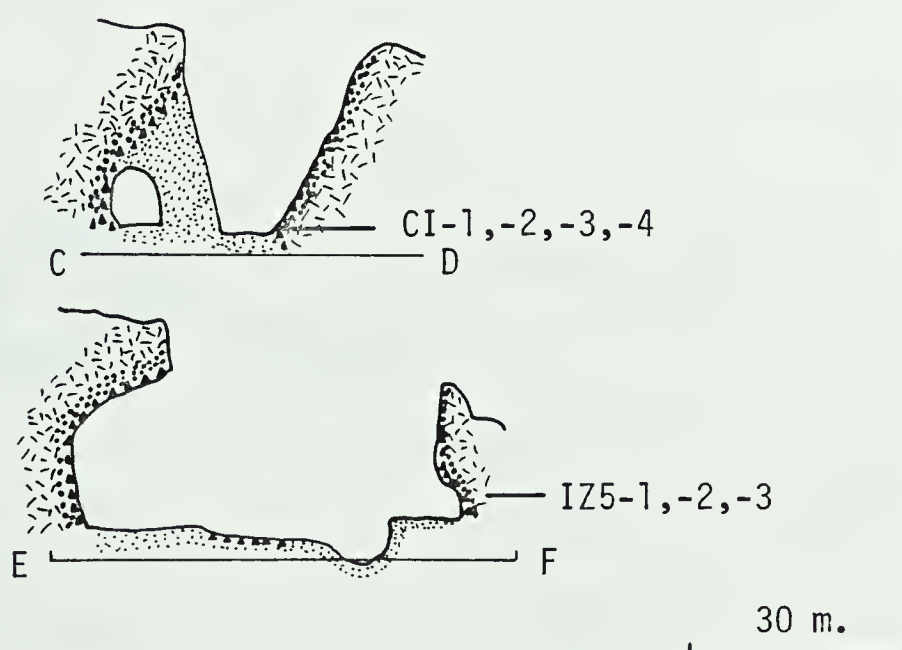
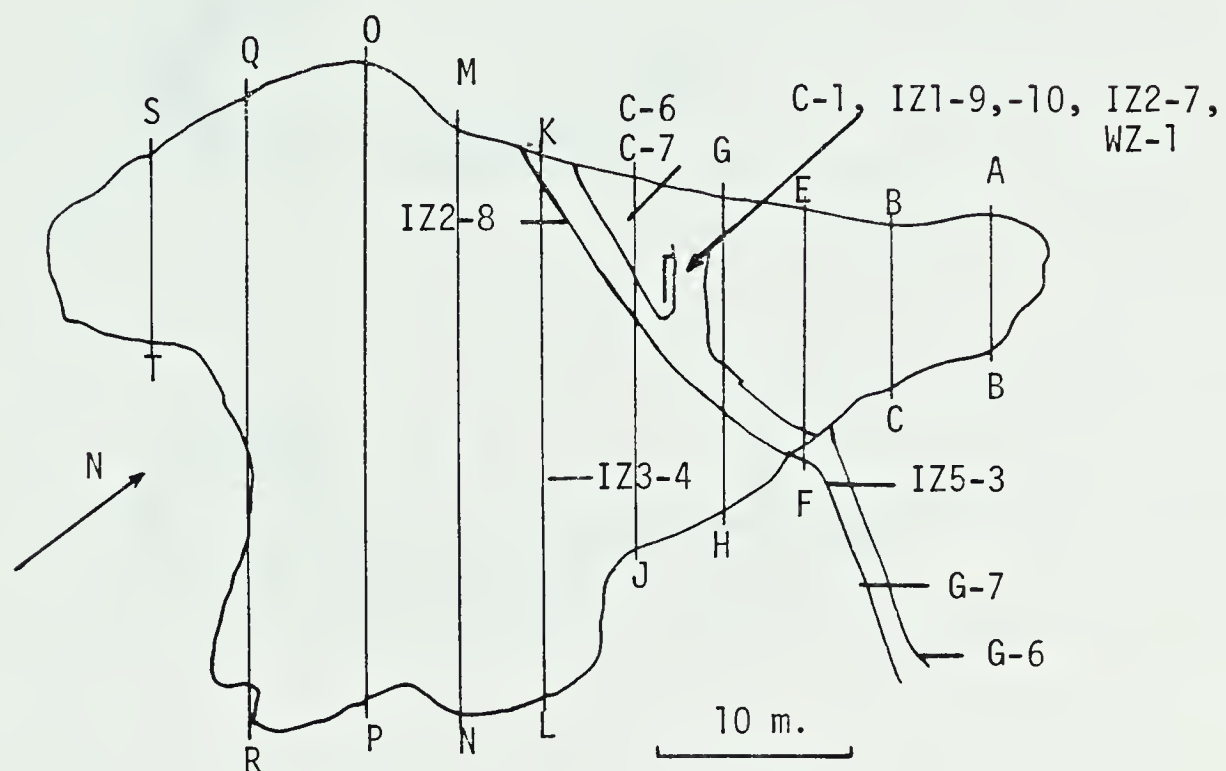
### CORE ZONE

#### C-1 Quartz Location: near profile C-D

A large subhedral wedge-shaped crystal of smoky, translucent quartz, with mm. to cm. sized books of light green muscovite coating one surface.



FIGURE 8. The Gloserheia Pegmatite; map of quarry. A-B to S-T are profiles. (After Amli, 1977).



Profiles C-D and E-F.



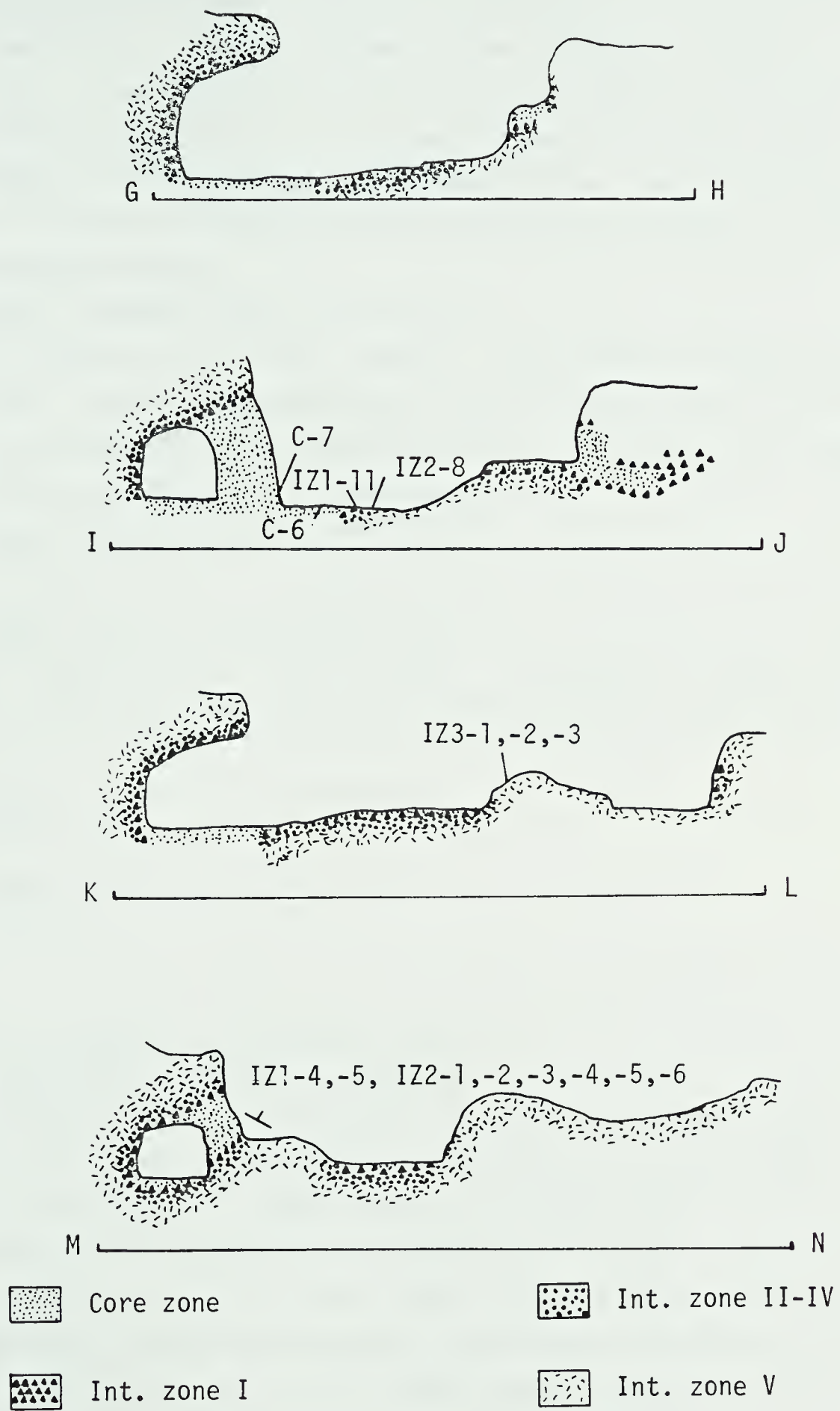


FIGURE 8. Continued.  
Profiles G-H to M-N





C-2 Microcline-perthite Location: near profile C-D

A large potassium feldspar crystal. The feldspar is visibly perthitic, and salmon pink in colour. One face of the crystal is lightly sericitized. Examination of the thin section reveals pronounced grid-iron twinning characteristic of microcline and string-type perthite. The feldspar is fractured and lightly sericitized. Local recrystallization of the microcline has occurred along the fractures in fine to medium-grained patches.

C-3 Quartz Location: near profile C-D

A large, anhedral milky quartz crystal. The crystal is moderately fractured. Thin section examination reveals dusty, microcrystalline opaque inclusions and the strained nature of the quartz, with undulatory extinction and sutured grain boundaries.

C-4 Quartz Location: near profile C-D

Similar to C-3

C-5 Quartz Location: near profile C-D

A large, anhedral, milky quartz crystal. The crystal is moderately fractured and a thin coating of fine-grained muscovite has developed on one face.

C-6 Quartz Location: profile I-J

Similar to C-5.

C-7 Quartz Location: profile I-J

Similar to C-5.

BOUNDARY OF CORE WITH INTERMEDIATE ZONE ICI-1 Quartz-Biotite-Microcline-Apatite Location: near profile C-D

A coarse-grained sample of subhedral perthitic microcline, quartz, apatite, and biotite. The apatite is a single pale green crystal. The single quartz crystal is smoky, translucent, and highly fractured. The microcline is visibly perthitic, salmon pink in colour, lightly sericitized and moderately fractured. The biotite is shiny and black, but the sheets are crenulated and possess two distinct cleavages; the second perpendicular to the usual perfect basal cleavage. There is local hematitic staining along the biotite-feldspar boundary.

Microscopic examination reveals bending of the twin lamellae and the moderately sericited nature of the microcline (sericite after microcline



apprx. 12%). The quartz is also visibly strained, with pronounced undulatory extinction and escalloped grain boundaries. The biotite is weakly cataclastic along the feldspar grain boundary. Undulatory extinction and kink banding are well developed, and the biotite is locally recrystallized.

CI-2 Biotite Location: near profile C-D

Several large books of biotite. The surfaces of the books are lightly chloritized, but the interiors are fresh and shiny in appearance. A second cleavage, perpendicular to the common basal cleavage, is well developed. The biotite sheets are slightly crenulated. The biotite is brittle in character rather than flexible and elastic.

CI-3 Apatite Location: near profile C-D

Large anhedral crystals, light green to grey green in colour. The crystals are moderately fractured, and the colour is bleached over a distance of several mm. in either direction along the fractures. Thin section examination shows microcrystalline inclusions of a fine dusty opaque (possibly hematite) and carbonate, especially along the fractures.

CI-4 Microcline perthite Location: near profile C-D

Large, visibly perthitic blocky crystal of microcline. It is salmon pink in colour and fresh in appearance.

INTERMEDIATE ZONE I

IZ1-1 Orthite

A large, wedge-shaped crystal, dark in colour with a pitchy lustre and metamict appearance. A reddish-brown surface alteration occurs on two faces. The sample is fractured, with a narrow zone of visible alteration along the fractures. In thin section the orthite is isotropic and highly altered, with abundant inclusions of a fine-grained oxide (dominantly hematite), a mica, and epidote or zoisite. The alteration is concentrated along the numerous anastomosing fractures.

IZ1-2 Quartz

Similar to C-5.

IZ1-3 Biotite

Similar to CI-2.

IZ1-4 Muscovite replacement pod

Highly altered plagioclase replaced by quartz and muscovite. The rock is



metasomatized in appearance and crumbles easily. The plagioclase is white and sugary in appearance, with patchy hematite staining. Deep green muscovite has replaced approximately 40% of the plagioclase. The replacement occurs as fine to medium-grained plates planar in orientation. One surface of the feldspar is coated by stubby, subhedral quartz crystals and coarse-grained dark green muscovite books up to 1 cm. in diameter and in thickness.

In thin section the oligoclase ( $An_{17}Ab_{83}$ ) has a clouded, turbid appearance with patchy extinction and poorly developed twinning. It is partially replaced by muscovite (about 35%) and subordinate carbonate (7%) and hematite (4%). Alteration is pronounced along fractures and cleavage traces. The muscovite is coarse-grained and is visibly strained with warped cleavages and undulatory extinction.

IZ1-5 Microcline perthite Location: near profile M-N

Similar to C-2. Thin section examination reveals a fresh, unaltered appearance. The microcline is a vein-type perthite, with local patches of string perthite. Trace local sericitization has developed along the borders of the albite veins.

IZ1-6 Xenotime

Microcrystalline (about 325 mesh) loose needles of pale yellow xenotime.

IZ1-7 Rutile

A dark brown metallic euhedral single crystal approximately 1 cm. in size.

IZ1-8 Oligoclase-Euxenite Location: border between Int. zones I & II

A coarse-grained intergrowth of plagioclase and euxenite. The plagioclase is lightly sericitized and shows patchy iron oxide staining. The euxenite occurs as subhedral to euhedral vitreous black crystals concentrated along a fracture band in the plagioclase.

Thin section examination reveals the turbid, sericitized nature of the oligoclase ( $An_{18}Ab_{82}$ ). The oligoclase comprised about 64% of the thin section. The twin lamellae are bent and deformed, and the grains show patchy extinction. The euxenite (12%) is isotropic. It is concentrated along a fracture band, and is associated with minor muscovite (6%), chloritized biotite (5%), carbonate (4%), hematite (9%), and an unidentified yellowish-brown alteration product (1%). Fractures radiate away from the euxenite into the enclosing feldspar, and fine-grained hematite







appears to fill most of these narrow cracks.

IZ1-9 Microcline perthite

Similar to C-2.

IZ1-10 Sericitized oligoclase

Similar to IZ1-4.

IZ1-11 Quartz-Biotite-Microcline

Similar to CI-1; no apatite.

INTERMEDIATE ZONE II

IZ2-1 Muscovite-Quartz

Loose small euhedral muscovite books and subhedral stubby quartz crystals. The crystals range between 1 and 3 cm. in size. The muscovite is fresh in appearance, pale green in colour and visibly zoned. The quartz is milky and translucent.

IZ2-2 Muscovite replacement pod Location: profile K-L

Similar to IZ1-4. Muscovite forms a thick crust on highly muscovitized plagioclase. The plagioclase is sugary in appearance and is highly porous. In thin section the feldspar is a chessboard mesoperthite and comprises about 63% of the thin section. Twinning is absent to poorly developed. Fine-grained muscovite and sericite after feldspar comprise about 32%. Alteration is especially pronounced along cleavage plains and fractures. Fine-grained hematite (about 3%) is concentrated along fractures and at grain boundaries.

IZ2-3 Muscovite replacement pod Location: profile K-L

Similar to IZ1-4. In thin section the coarse-grained feldspar (about 57%) is turbid and locally replaces muscovite (26%) and fine to coarse-grained carbonate (8%). The feldspar is a chessboard mesoperthite and is graphically intergrown with coarse-grained quartz. The quartz is visibly strained, with polygonal texture and undulose extinction. The muscovite grades in size from fine-grained sericite to large euhedral plates. The cleavages are bent and deformed, and extinction is undulose.

IZ2-4 Oligoclase

A coarse-grained anhedral intergrowth of plagioclase cut by a narrow quartz grain. The plagioclase is pale green in colour and is visibly sericitized. In thin section, oligoclase ( $An_{18}Ab_{82}$ ) is replaced by fine-grained muscovite (about 38%). Carbonate alteration (4%) is locally



developed along fractures.

IZ2-5 Biotite Location: south wall

Similar to CI-2.

IZ2-6 Muscovitized oligoclase

An anhedral intergrowth of coarse-grained plagioclase. The plagioclase has been highly muscovitized with replacement by medium-grained quartz and carbonate. Light patchy hematite staining is visible along fractures and on the rock surface.

In thin section, the relic feldspar comprised about 24%. The primary oligoclase ( $An_{18}Ab_{82}$ ) appears to have been incompletely replaced by a chessboard mesoperthite. Quartz (32%) is polygonized with undulose extinction and occurs dominantly in a graphic-textured and locally myrmekitic intergrowth with the perthite. Fine to medium-grained carbonate (8%) is present as an oligoclase replacement, and hematite (2%) is concentrated in the carbonate and along fractures.

IZ2-7 Oligoclase Location: between profiles G-H and I-J.

An intergrowth of coarse-grained subhedral (presumed) oligoclase. The plagioclase is fresh in appearance but has a light green, weathered outer rind about 5 mm. in thickness. Fracture surfaces are lightly sericitized.

IZ2-8 Oligoclase-Quartz Location: profile I-J

Similar to IZ2-4.

### INTERMEDIATE ZONE III

IZ3-1 Plagioclase- $\beta$ -uranophane

An intensely altered plagioclase with abundant medium-grained muscovite, carbonate, and hematite. Highly fractured with local development of small, powdery lemon-coloured pockets of  $\beta$ -uranophane.

IZ3-2 Perthite-Euxenite Location: profile K-L

An intergrowth of coarse-grained sericitized feldspar, glossy black euxenite and laths of chloritized biotite.

In thin section the feldspar comprises about 56%. The high degree of sericitization masks the relationship between the feldspar phases. Orthoclase appears to have replaced oligoclase in a replacement-type perthite pattern. Twinning in the plagioclase is only faintly visible, and the



anorthite content is indeterminate. Sericitization (about 32%) is concentrated in the plagioclase (presumed oligoclase). Fine-grained carbonate (6%) forms a replacement for feldspar in intimate association with euxenite. The medium-grained blocky euxenite (4%) is isotropic and has formed radiating fractures in the adjacent phases. Micro-crystalline hematite and other oxides (4%) are concentrated along fractures and at grain boundaries.

#### IZ3-3 Oligoclase-Biotite-Euxenite-Quartz-Sphene

A coarse-grained intergrowth of red plagioclase, hexagonal books of biotite, glossy black euxenite, and single subhedral crystals of quartz and sphene. The quartz, euxenite, biotite and sphene appear to form a wide vein in the highly hematized feldspar. The thin section was cut through this 'vein'.

In thin section, highly sericitized oligoclase ( $An_{16}Ab_{84}$ ) comprises approximately 26%, with sericite after oligoclase 34%. It is moderately fractured, with fine-grained hematite (11%) and carbonate (4%) concentrated along these fractures causing the bright red colour. A large subhedral equant crystal of sphene (11%) appears to be rimmed by biotite. The biotite (12%) is extensively chloritized with lamellar intergrowths of quartz (2%) and carbonate (2%) concordant with and interstitial to the cleavage.

IZ3-4 Oligoclase-Euxenite Location: between profiles I-J and K-L  
Similar to IZ3-2.

### INTERMEDIATE ZONE IV

#### IZ4-1 Microcline-Oligoclase-Biotite Location: profile K-L

Coarse-grained intergrowth of anhedral feldspar and randomly oriented biotite laths. Light hematite staining is present along fractures. In thin section, oligoclase (19%) is turbid and lightly sericitized (sericite after oligoclase 11%) and apparently partially replaced by microcline (28%). At interfaces the oligoclase is scalloped and embayed and contains minor myremekite. In contrast, the microcline is fresh in appearance but contains narrow lenses of fine-grained clays and sericite in subordinate amounts in a perthitic intergrowth parallel to the dominant fracture pattern. Quartz (33%) forms a graphic intergrowth with the feldspar and is strained in appearance, with pronounced







undulatory extinction. Chlorite (3%) has partially replaced the biotite laths (5%) with trivial local alteration to muscovite (1%).

IZ4-2 Microcline-Oligoclase-Biotite Location: profile K-L

Similar to IZ4-1. The grain size is slightly larger, and there is slightly greater apparent replacement of oligoclase ( $An_{12}Ab_{88}$ ) by microcline

INTERMEDIATE ZONE V

IZ5-1 Microcline perthite-Quartz

Graphic-textured intergrowth of microcline perthite and quartz. The feldspar and quartz are medium to coarse-grained and anhedral. The feldspar is lightly sericitized and hematite staining is visible along fracture planes. In thin section the vein-type microcline perthite is very lightly sericitized, with sericite after feldspar comprising about 4%. The quartz (32%) is strained.

IZ5-2 Perthite-Quartz

A large feldspar crystal, lightly sericitized, with graphically intergrown quartz. Minor hematite staining gives the feldspar a pale pink colour.

In thin section, orthoclase (35%) appears to be replacing plagioclase (19%) in a replacement-type perthite pattern. The orthoclase is relatively fresh in appearance, but locally has a ghost-like suggestion of lamellar twinning. Relict patches of plagioclase are very slightly better twinned, and are heavily sericitized, with fine-grained muscovite and sericite after plagioclase comprising about 28%. Fine-grained hematite and oxides (6%) are concentrated along fractures and cleavages.

IZ5-3 Oligoclase-Quartz Location: profile G-F

A coarse-grained intergrowth of equal portions of quartz and plagioclase (presumed oligoclase). Smoky, translucent quartz occurs in anhedral rods in an approximation of graphic texture. Quartz and blocky oligoclase are hematite stained along fracture surfaces and cleavages. The oligoclase is otherwise relatively fresh in appearance. Coarse-grained cavities partially filled by chlorite probably represent the remnants of large biotite books.



## WALL ZONE

WZ-1 Microcline perthite-Quartz Location: between profiles G-H & I-J  
Similar to IZ5-1, but more coarse-grained in texture.

### WZ-2 Oligoclase-Euxenite-Quartz

A coarse-grained intergrowth of chalky oligoclase and randomly dispersed tabular glossy black euxenite. The sample is highly fractured with pronounced hematite staining and powdery lemon yellow coloured pockets of uranium secondaries.

In thin section, the advanced sericitization of the plagioclase renders the composition indeterminate. Alteration products after (presumed) oligoclase include sericite (34%) and fine-grained carbonate (12%) and muscovite (6%). The euxenite is metamict and has caused radiating fractures in the enclosing feldspar. Fine-grained hematite (8%) is concentrated along fractures.

### WZ-3 Oligoclase-Quartz-Biotite-Kasolite

A medium to coarse-grained sample of highly sericitized blocky oligoclase stubby quartz and books of biotite. Small pockets and fractures are respectively filled with fine acicular and powdery ocher-yellow coloured crystals of kasolite. The biotite is visibly chloritized and the feldspar and quartz are hematite stained.

## BORDER ZONE

BZ-1 Oligoclase-Quartz Location: profile E-F, near F  
Coarse-grained graphic intergrowth of quartz and plagioclase. The tabular, subhedral plagioclase grades into patchy pink feldspar along fractures. Fractures are hematite stained.

## COUNTRY ROCK

G-6 Amphibolite Location: North side of tunnel entrance

A fine-grained sample of fresh, equigranular amphibolite showing weakly developed foliation. Equant plagioclase grains (24%) have a relatively sodic composition ( $An_{17}Ab_{83}$ ) and show well-developed albite twinning. Anhedral microcline has well developed tartan twinning and forms a minor constituent (5%). Granular quartz comprises 19%. Hornblende is the most abundant mineral phase (27%). Subhedral prismatic forms show



characteristic ragged terminations. Wedge-shaped crystals of sphene comprise 12%. Chlorite (9%) completely replaces an unidentified constituent. Minor accessories are an opaque (4%) and apatite (2%).

G-7 Amphibolite Location: south side of tunnel

Similar to G-6. Slightly more coarse-grained. Hornblende shows poorly developed sieve texture.





## APPENDIX B: MINERAL SEPARATION PROCEDURES

The rocks were washed and dried. All of the equipment to be used was thoroughly cleaned initially and between samples to minimize the possibility of contamination.

A suitably sized portion of each sample was split off and passed through a jaw crusher. This coarse-grained material was then fed through a disc grinder. A percussion mortar was used to crush very small sample samples. The material was then washed and sieved and the -35 +80 fraction was isolated and retained.

This rock powder was fed through a Franz Isodynamic separator until the purest possible mineral separates were obtained. These fractions were further purified with the use of heavy liquids. Methylene iodide (S.G. about 3.3) was used to obtain homogenous fractions of muscovite and of biotite and to separate euxenite from less dense silicate components. Tetrabromethane (S.G. about 2.8) was used to obtain homogenous gravity fractions of feldspar and quartz. The heavy liquids were diluted with the gradual addition of acetone to obtain a density gradient within the separatory funnel. It was generally found that the major portion of each mineral separate possessed a narrow range in specific gravity, and this portion was retained for isotope analysis. Several of the feldspars showed a strongly bimodal distribution in specific gravity. In these cases the two fractions were selected for analysis. Because of the perthitic nature of the feldspars and the variation in the Rb/Sr ratios of the two fractions it is believed that the denser fraction represents the enrichment of the sodic phase of the perthite while the lighter fraction represents the enrichment of the potassic phase.

The mineral separates were visually inspected for purity with a binocular microscope and then stored in clean labelled plastic vials.

Total rock samples were split from the original sample and then passed through the jaw crusher and disc grinder. This powder was then crushed to a very fine powder in a Tema swing mill. The powders were stored in clean labelled plastic vials.



## APPENDIX C: ANALYTICAL TECHNIQUES

### i. Rubidium-Strontium.

Rubidium and strontium determinations were carried out on muscovite, biotite, plagioclase and microcline using the isotope dilution method (see Faure, 1977, for a detailed description).

The samples were analysed by XRF to determine the approximate abundance of Rb and Sr. A quantity of feldspar estimated to contain 20 micrograms of Sr, or 1 gram of sample in the case of mica, was mixed in a teflon beaker with about 1 gram of a spike solution containing both Rb and Sr. Choice of one of two prepared spike solutions (containing either 2 ug/g  $^{84}\text{Sr}$  and 200 ug/g  $^{87}\text{Rb}$  or 2 ug/g  $^{84}\text{Sr}$  and 5.5 ug/g  $^{87}\text{Rb}$ ) was based on the Rb/Sr ratio of the sample. Samples having a ratio of less than 1 were mixed with the low Rb spike. Otherwise the spike with the higher ratio was used, because it was more similar in composition to the samples.

To this mixture 10 ml. each of concentrated vapor distilled HF and  $\text{HNO}_3$  were added. The beaker was covered and heated a minimum of 8 hours to equilibrate and decompose. The solution was uncovered and evaporated to dryness. The residue was moistened with water and 5 ml.  $\text{HNO}_3$  and evaporated to dryness. This step was repeated at least once. 5 ml. of  $\text{HNO}_3$  and 30 ml. of water were added, and the solution was covered and heated for about 4 hours. The solution was uncovered and evaporated to about 10 ml. If a precipitate was present at this time the contents of the beaker were transferred to a teflon test tube and centrifuged. The supernate was decanted into a 50 ml. silica glass centrifuge tube containing about 10 mg. of Sr-free  $\text{Ba}(\text{NO}_3)_2$  solution.  $\text{HNO}_3$  was added slowly with stirring until a copious precipitate of  $\text{Ba}(\text{NO}_3)_2$  collected at the base of the tube. The solution was centrifuged. The supernate, containing the Rb, was decanted. The precipitate containing the Sr was saved.

For Rb, the supernate was poured into a platinum dish containing 0.5 ml. of vapor distilled concentrated  $\text{H}_2\text{SO}_4$ . The solution was evaporated to dryness and then ignited at  $900^\circ\text{C}$ . The residue was leached with 0.5 ml. of water, and the K and Rb were reprecipitated with concentrated





HClO<sub>4</sub>. After centrifuging the supernate was discarded and the precipitate was redissolved in a drop of hot water. A drop of this saturated solution was loaded on the side filament of an outgassed double filament for analysis on a mass spectrometer.

For Sr, the Ba(NO<sub>3</sub>)<sub>2</sub> precipitate was dissolved in a minimum of water and reprecipitated with the addition of HNO<sub>3</sub>. The precipitate was redissolved and reprecipitated several times. The precipitate was dried and then redissolved in 0.5 ml. of vapor distilled 2.3 N HCl. This solution was loaded onto a pre-calibrated Dowex cation exchange column and eluted with 2.30 N HCl. The Sr eluate fraction was collected and evaporated to dryness. The residue was dissolved in 2.3 N HCl and loaded onto the side filament of an outgassed double Rhenium filament for analysis on a mass spectrometer.

## ii. Uranium-Lead

Euxenite and xenotime were analysed for uranium and lead isotopic composition using the isotope dilution (ID)/isotope ratio (IR) method described by Krogh (1973). 2 mg. of euxenite or 35 mg. of xenotime (weights were chosen for optimum spiking ratios) were weighed into teflon bombs. The samples were equilibrated and decomposed by addition of 10:1 concentrated vapor distilled HF and HNO<sub>3</sub>. The bombs were heated at 165<sup>0</sup> for 48 hours. The solutions were then evaporated to dryness. The residues were moistened with 1:1 HNO<sub>3</sub> and H<sub>2</sub>O, and then heated at 130<sup>0</sup>C for 48 hours. The bombs were cooled and weighed. Half the solution was poured into a weighed silica beaker containing 10 ml. of <sup>238</sup>U spike solution. One gram of <sup>208</sup>Pb spike was weighed into the beaker. This aliquot was used for ID determination of U and Pb.

The remainder of the unspiked solution was used for IR measurement. This was processed in the same manner as the lead ID sample.

The IR aliquot was concentrated through evaporation. Lead-free Ba(NO<sub>3</sub>)<sub>2</sub> was added to separate U from Pb using the barium coprecipitation method. The lead coprecipitated with the Ba(NO<sub>3</sub>)<sub>2</sub> leaving the U in solution. After centrifuging, the supernate was transferred to a teflon beaker and evaporated to dryness. The U was further purified through elution on a nitrate-anion exchange column with HNO<sub>3</sub>. The U-bearing eluate was dried and then loaded in a drop of HNO<sub>3</sub> on the side filament





of an outgassed double rhenium filament.

The Pb, coprecipitated as a nitrate, was further purified through elution on a chloride anion-exchange column with HCl. The Pb-bearing eluate was dried and then loaded in a drop of  $\text{H}_3\text{PO}_4$  on a film of silica gel on the center filament of an outgassed double rhenium filament.











**B30298**